

**Special Section: Remote Sensing
for Vadose Zone Hydrology**

W.A. Dorigo*
A. Xaver
M. Vreugdenhil
A. Gruber
A. Hegyiová
A.D. Sanchis-Dufau
D. Zamojski
C. Cordes
W. Wagner
M. Drusch



The International Soil Moisture Network contains more than 6100 in situ soil moisture data sets from all over the world to support the development of remote sensing products and land surface models, and to facilitate studying the behavior of our climate over space and time. We present a new, automated quality control system for these measurements.

W.A. Dorigo, A. Xaver, M. Vreugdenhil, A. Gruber, A. Hegyiová, A.D. Sanchis-Dufau, D. Zamojski, C. Cordes, and W. Wagner, Dep. for Geodesy and GeoInformation, Vienna Univ. of Technology, Vienna, Austria; M. Drusch, European Space Agency, ESTEC, Noordwijk, the Netherlands. *Corresponding author (wd@ipf.tuwien.ac.at).

Vadose Zone J.
doi:10.2136/vzj2012.0097
Received 1 July 2012.

© Soil Science Society of America
5585 Guilford Rd., Madison, WI 53711 USA.
All rights reserved. No part of this periodical may
be reproduced or transmitted in any form or by any
means, electronic or mechanical, including photo-
copying, recording, or any information storage
and retrieval system, without permission in writing
from the publisher.

Global Automated Quality Control of In Situ Soil Moisture Data from the International Soil Moisture Network

The International Soil Moisture Network (ISMN) was initiated in 2009 to support calibration and validation of remote sensing products and land surface models, and to facilitate studying the behavior of our climate over space and time. The ISMN does this by collecting and harmonizing soil moisture data sets from a large variety of individually operating networks and making them available through a centralized data portal. Due to the diversity of climatological conditions covered by the stations and differences in measurement devices and setup, the quality of the measurements is highly variable. Therefore, appropriate quality characterization is highly desirable for a correct use of the data sets. This study presents a new, automated quality control system for soil moisture measurements contained in the ISMN. Two types of quality control procedures are presented. The first category is based on the geophysical dynamic range and consistency of the measurements. It includes flagging values exceeding a certain threshold and checking the validity of soil moisture variations in relation to changes in soil temperature and precipitation. In particular, the usability of global model- or remote sensing-based temperature and precipitation data sets were tested for this purpose as an alternative to in situ measurements, which are often not recorded at the soil moisture stations themselves. The second category of procedures analyzes the shape of the soil moisture time series to detect outliers (spikes), positive and negative breaks, saturation of the signal, and unresponsive sensors. All methods were first validated and then applied to all the data sets currently contained in the ISMN. A validation example of an AMSR-E satellite and a GLDAS-Noah model product showed a small but positive impact of the flagging. On the basis of the positive results of this study we will begin to add the flags as a standard attribute to all soil moisture measurements contained in the ISMN.

Abbreviations: CMAP, Climate Prediction Center's operation global 2.5° 5-d Merged Analysis of Precipitation; HWSD, Harmonized World Soil Database; ISMN, International Soil Moisture Network; NRT, near real time; QC, quality control.

Ground-based measurements of soil moisture have been widely used for validating remote sensing-based soil moisture products (e.g., Gruhier et al., 2010; Jackson et al., 2010; Liu et al., 2011; Parrens et al., 2012; Pathe et al., 2009; Zribi et al., 2009), calibrating and validating model estimates of soil moisture and drought (Balsamo et al., 2009; Dai et al., 2004; Rodell et al., 2004), and studying the dynamics of soil moisture in space and time (Albergel et al., 2008; Brocca et al., 2010; Entin et al., 2000; Famiglietti et al., 2008). Worldwide, a large number of local to regional-scale meteorological and experimental networks are available for these tasks. However, in many cases it is difficult to gain access to these data sets. Besides, there is general lack of standardization of methods and protocolling which complicates the combined use of multiple networks in global studies. To overcome many of these limitations, the International Soil Moisture Network (<http://www.ipf.tuwien.ac.at/insitu>) was initiated in 2010 to serve as a centralized data hosting facility where globally available in situ soil moisture measurements from operational networks and validation campaigns are collected, harmonized, and made available to users through a single access point (Dorigo et al., 2011a,b). Currently, the ISMN contains more than 6100 soil moisture data sets from over 1400 stations available through 35 different networks. The scientific relevance of this centralized and harmonized system is reflected by the growing number of studies that use a combination of networks to evaluate soil moisture products at a continental to global scale (e.g., Albergel et al., 2012; Brocca et al., 2011; Liu et al., 2012).

The data sets shared with the ISMN are very heterogeneous in terms of measurement technique, measurement depth, spatial setup, and degree of automation. While incoming data sets are harmonized in terms of soil moisture unit, time stamp, and metadata,

the ISMN does not perform a homogenization over depth and between different sites. Besides, little is known about the quality of the individual measurement time series. The quality of individual sites is mainly a result of measurement device used, deployment of the sensor in the field, and its calibration (Bogena et al., 2007; Mittelbach et al., 2011). A quantitative estimate of the relative quality of stations is of particular interest to those who wish to draw conclusions on the performance of a product based on a validation over a variety of networks. Hence, quality assurance has become one of the major concerns of the Committee on Earth Observation Satellites (CEOS) Land Product Validation (LPV) group (<http://lpvs.gsfc.nasa.gov/>, accessed 28 Nov. 2012), whose objective is to develop guidelines for validation of satellite-based soil moisture products such as provided by ASCAT (Bartalis et al., 2007), AMSR-E (Owe et al., 2008), SMOS (Mecklenburg et al., 2012), and SMAP (Entekhabi et al., 2010). However, not only at the station level, but also at the level of the individual measurements quality control (QC) is an important issue, as quality can vary strongly between the readings. Whereas smaller, experimental networks may have the resources and time to perform a visual QC on their data, this is infeasible for large automated networks that share their data in near real time (NRT). Hence, automated objective methods are needed.

Methods for automated QC are widespread in various geophysical disciplines, such as in air temperature and precipitation monitoring (Hubbard et al., 2005), solar radiation (Journée and Bertrand 2011), sea surface temperature (González-Rouco et al., 2001; Merchant et al., 2008), and ocean salinity (Ingleby and Huddleston, 2007). The most common methods for outlier detection are based on thresholds that can either be static or variable over time (Journée and Bertrand 2011). Others derive thresholds from statistical properties of the data set, such as mean, standard deviation, or quartiles (González-Rouco et al., 2001; Merchant et al., 2008). To do so, reliable climatologies based on long measurement time series are required (Hubbard et al., 2005). Spectrum-based approaches study the shape of a measured time series to identify potential outliers. The most prominent members of this category are spike detection algorithms (Malyshev and Sudakova, 1995; Meinander et al., 2003; Ossadtchi et al., 2004). Spikes are typically defined as unanticipated significant rises or drops lasting only one time step. As their maxima can occur within plausible physical ranges they often remain undetected by threshold-based approaches. Recently, researchers have proposed several sophisticated statistical spike detection methods based on parametric methods, clustering techniques, neural networks, and wavelets (Farrokhi et al., 2010; Inan and Kuntalp, 2007; Torrence and Compo, 1998). The availability of a gap free time series that is long enough is critical for a robust use of wavelets because wavelet transforms applied to short time series may lead to boundary effects (Nenadic and Burdick, 2005). Dense observing networks allow for the use of buddy checking methods (Rayner et al., 2006). The main idea behind this technique is the assumption that nearby measurements display similar

dynamic behavior in time. If an outlier in one measured time series cannot be supported by its buddies, then the data point is most likely incorrect. Critical for the application of the buddy technique is the presence of enough neighboring observations at distances showing significant spatial correlation. With growing data availability from multiple sources, probability-based approaches become an increasingly interesting alternative for detecting errors. For example, Ingleby and Huddleston (2007) used a Bayesian framework based on different information sources to check for the plausibility of ocean temperature and salinity values. Typically, spurious observations detected by a quality control procedure are flagged. Flagging is a procedure that adds a quality indicator to the original observation but without modifying or removing it from the data set. This leaves it up to the user or application to decide what to do with the flagged observation.

To date, automated QC of in situ soil moisture data has received only little attention in literature. Illston et al. (2008) and You et al. (2010) used several variations of threshold-based approaches to flag spurious observations. In addition, You et al. (2010) used a spatial regression test to identify measurements that deviated from a regional soil moisture model (Hubbard et al., 2005). Though thoroughly addressing the QC issue, the studies focus on a single network for which the measurement setup is relatively consistent among the various sites (Illston et al., 2008; You et al., 2010). A first simple QC procedure at a global level for the data sets of the ISMN was proposed by Dorigo et al. (2011b) who applied several physically based thresholds to flag spurious observations according to the Coordinated Energy and Water Cycle Observations Project (CEOP) Data Flag Definitions (http://www.eol.ucar.edu/projects/ceop/dm/documents/refdata_report/data_flag_definitions.html, accessed 28 Nov. 2012). However, the system appeared insufficient for flagging more subtle outliers.

This study builds on existing experiences in the field of QC for in situ soil moisture data and proposes a comprehensive automated QC system for the ISMN. The major challenge is to define an objective QC system that is applicable to a large variety of networks and stations that differ strongly in nature and available metadata. The manuscript starts with a general description of the ISMN and a more detailed description of the data sets that are used for developing and testing the QC procedures (data description). To be able to detect potential errors, first the natural appearance of soil moisture measurements and deviations from this natural behavior need to be understood (“Sources and Appearance of Errors in In Situ Soil Moisture Measurements”). An overview of the QC methods is presented in the “Quality Control Methods” section, followed by an evaluation and discussion of the QC, based on a validation subset and application to the entire ISMN (“Results and Discussion”). Also, an example of the effect of flagging on validating remotely sensed and modeled soil moisture is provided in this section.

Data Description

The methods presented in this study were developed and validated using data from the ISMN (Dorigo et al., 2011a,b). At the time of writing (November 2012) the ISMN hosted 35 networks representing more than 1400 measurement stations, mostly clustered in the United States and Eurasia (Fig. 1). A network is defined as any number of stations managed by a single organization or partnership. In practice, this number ranges between one and several hundred. It is important to realize that the networks have been designed for different applications and therefore show different characteristics and features. While all individual stations measure soil moisture many stations also provide measurements of variables that allow for a more comprehensive interpretation of the soil moisture data sets, including soil and air temperature, precipitation, and snow cover and depth (Table 1). In addition, the networks deploy different measurement techniques and sensors, including time and frequency domain reflectometry, capacitance and neutron probes, cosmic rays, and gravimetric sampling. All methods have their advantages and disadvantages for particular applications (Dorigo et al., 2011b; Robinson et al., 2008).

Figure 2 shows that temporal data availability varies from network to network. The networks that were transferred from the Global Soil Moisture Data Bank (Robock et al., 2000)—CHINA, MONGOLIA, IOWA, and the three RUSWET networks—are no longer updated and provide measurements only at irregular time intervals (typically 1–2 times per month). Therefore, these networks were excluded from most analyses in this study. All other

networks were considered. Recently, several networks have been added of which the data sets are updated automatically in near real time (ARM, COSMOS, FMI, SCAN, SNOTEL, SWEX_Poland, and USCRN). The data sets provided by these networks do not undergo any QC before being submitted to the ISMN. On the contrary, data from most other networks first undergo extensive visual quality inspection by the data providers before being shared with the ISMN. For an extensive overview of the single networks we refer to the supplemental material or to the original publications describing the networks (Table 1).

Sources and Appearance of Errors in In Situ Soil Moisture Measurements

Characteristic Behavior of Soil Moisture Readings

Fundamental for detecting errors in soil moisture measurements is a thorough understanding of their typical characteristics. Although it is unrealistic to speak of a single typical behavior of logged soil moisture (due to soil moisture regimes that vary dramatically across the globe), there are several features that most readings have in common. Figure 3a shows an example of a typical soil wetting event due to precipitation and the consecutive drying out. Such a characteristic curve is encountered in locations or periods with few precipitation events, so that enough time lies in between two consecutive precipitation events, thus allowing for a drying out until reaching asymptotically a quasi-stable soil water level (Hillel, 1998). If the dry period is long enough,

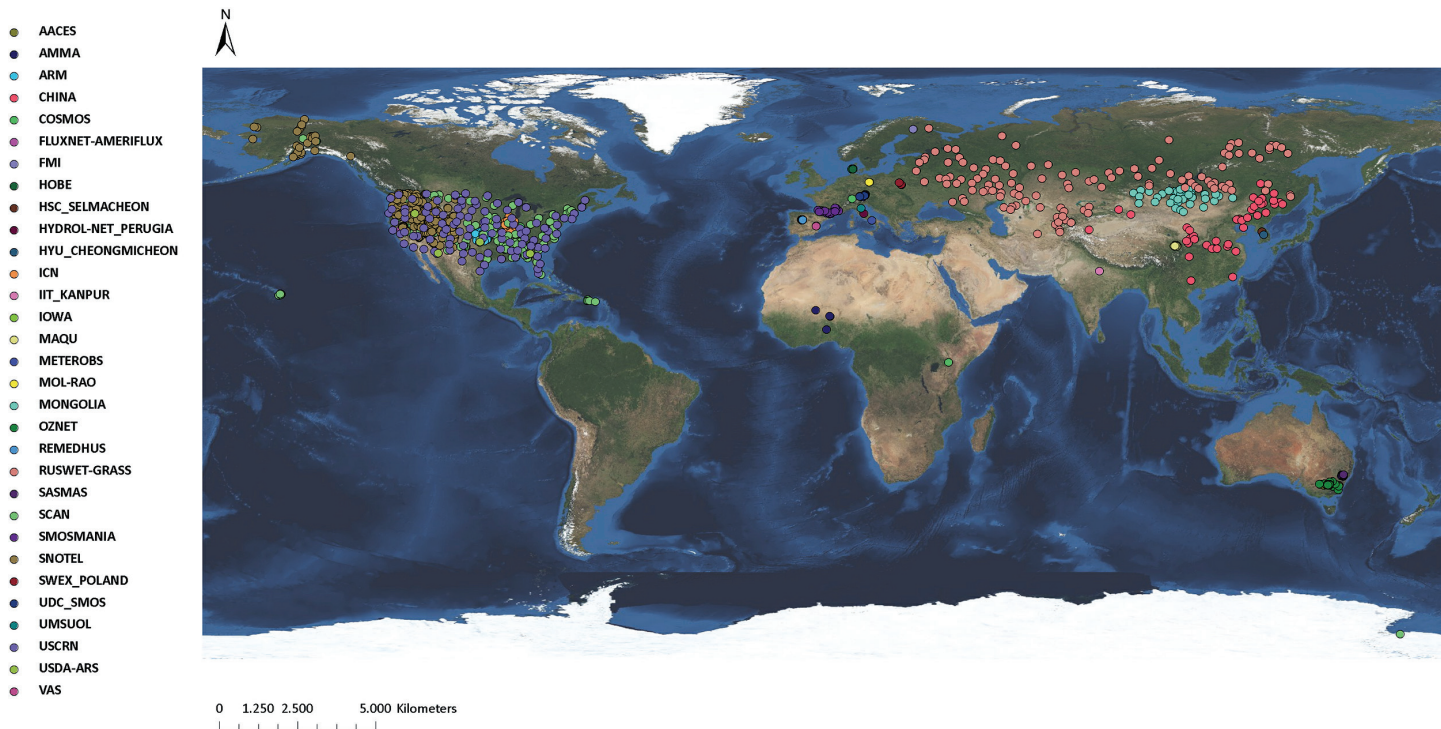


Fig. 1. Stations currently contained in the International Soil Moisture Network (status November 2012).

Table 1. Networks currently contained in the International Soil Moisture Network (ISMN) (status June 2012) and the measurements provided.[†]

Name	Stations	Variables included in ISMN	Operational status	Reference
AACES	49	SM (2), TS (4), P (1)	closed campaign	(Peischl et al., 2012)
AMMA	7	SM (13)	active	(Cappelaere et al., 2009; de Rosnay et al., 2009; Mougin et al., 2009; Pellarin et al., 2009)
ARM	25	SM (10), TS (10), TA (1), P	active	–
CALABRIA	5	SM (3), TA (1), P	active	(Brocca et al., 2011)
CAMPANIA	2	SM (1), TA (1), P	active	(Brocca et al., 2011)
CHINA	40	SM (11)	closed	(Robock et al., 2000)
COSMOS	56	SM (31)	active	(Zreda et al., 2008)
FLUXNET_AMERIFLUX	2	SM (8), TS (13), TA (1), P	active	–
FMI	1	SM (2), TS (1), TA (1)	active	(Rautiainen et al., 2012)
HOBE	30	SM (3), TS (3)	active	(Bircher et al., 2012)
HSC_SELMACHEON	1	SM (1)	active	–
HYDROL-NET_PERUGIA	1	SM (4), TS (2), TA (1), P	active	–
HYU_CHEONGMICHEON	1	SM (1)	active	–
ICN	19	SM (17), TS (6), P	active	(Hollinger and Isard 1994)
IIT_KANPUR	1	SM (4)	active	–
IOWA	6	SM (12)	closed	(Robock et al., 2000)
MAQU	20	SM (1), TS (1)	active	(Su et al., 2011)
MetEROBS	1	SM (5)	active	–
MOL-RAO	2	SM (9), TS (12), TA(2), P	active	(Beyrich and Adam 2007)
MONGOLIA	44	SM (10)	closed	(Robock et al., 2000)
OZNET (incl. SASMAS)	64	SM (7), TS (7), SS(7), P	active	(Rüdiger et al., 2007; Young et al., 2008)
REMEDHUS	23	SM (1), TS (1)	active	(Sanchez et al., 2012)
RUSWET-AGRO	156	SM (2)	closed	(Robock et al., 2000; Vinnikov and Yeserkepova 1991)
RUSWET-GRASS	122	SM (2)	closed	(Robock et al., 2000; Vinnikov and Yeserkepova 1991)
RUSWET-VALDAI	3	SM (3), TS (3), TA (2), P	closed	(Robock et al., 2000; Vinnikov and Yeserkepova 1991)
SCAN	182	SM (25), TS (25), TA (2), P, SD (1), SWE (1)	active	–
SMOSMANIA	21	SM (4)	active	(Albergel et al., 2008; Calvet et al., 2008)
SNOTEL	381	SM (16), TS, TA, P, SWEQ, SD	active	–
SWEX_POLAND	6	SM (8), TS (13)	active	(Marczewski et al., 2010)
UDC_SMOS	11	SM (5)	closed	(Loew et al., 2010)
UMBRIA [#]	7	SM (3), TA (2), P	active	(Brocca et al., 2011, 2008, 2009)
UMSUOL	1	SM (7)	active	(Brocca et al., 2011)
USCRN	113	SM (5), TS (5), TA (1), P (1), TSURF	active	(Bell et al., 2012)
USDA-ARS	4	SM (1), TS (2)	active	(Jackson et al., 2010)
VAS	3	SM(1), TS (6), TA(1)	active	–

[†] SM, soil moisture; TS, soil temperature, TSURF, surface temperature, TA, air temperature; P, precipitation; SD, snow depth, SWE, snow water equivalent; SS, soil suction. Numbers in parentheses are the number of layers (depths) at which the respective variable is provided.

[#] Previously listed as CNR_IRPI.

soil moisture content will eventually reach a constant value close to zero (for the surface layer) or another steady-state value (for deeper layers; Fig. 3a). In many cases, however, a new precipitation event takes place before stable soil moisture content is reached, leading to a superimposition of events that are difficult to discriminate (Fig. 3b).

A particular behavior of the measured soil moisture signal is registered for frozen soils and the cyclic behavior of freeze–thaw events (Fig. 3c). As the dielectric conductivity of ice is significantly lower than that of liquid water, the freezing of soil water leads to significantly lower recorded soil water content (Hallikainen et al., 1985).

During thaw periods, which are typically characterized by events of thawing (during daytime) and freezing (nighttime), alternating low and high levels of soil moisture are recorded that are not connected to precipitation events.

Most soil moisture measuring devices show a more or less pronounced sensitivity to temperature (Dorigo et al., 2011b; Robinson et al., 2008). In the frequency range where most electromagnetic in situ sensors and remote sensing systems operate (i.e., between ~ 0.001 and 10 GHz) there is a positive relationship between electric conductivity and temperature. This is reflected in Fig. 3d

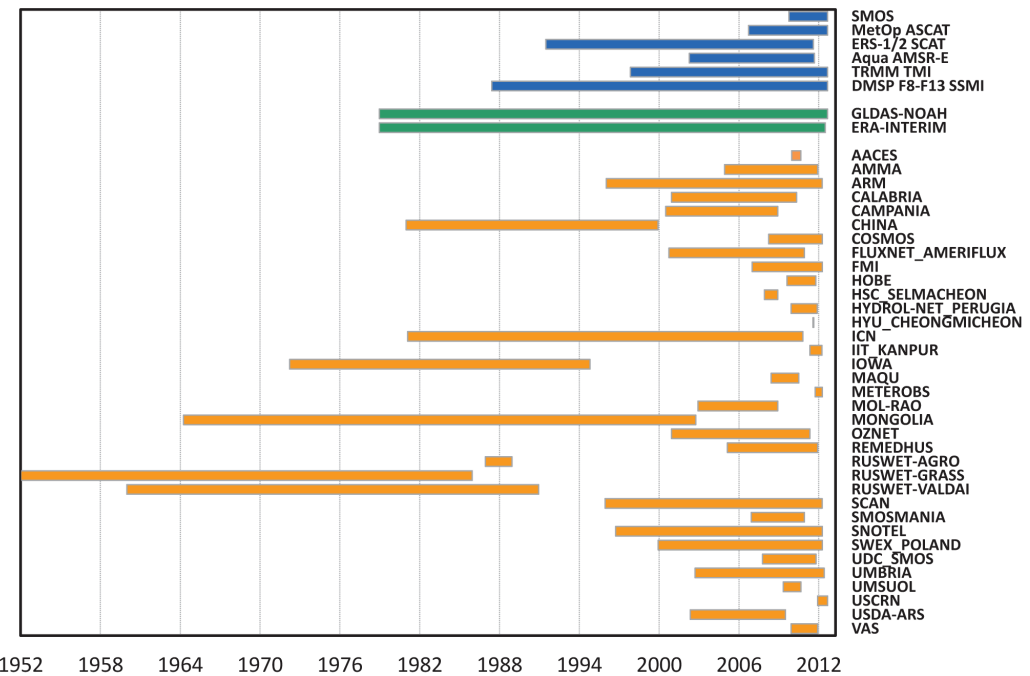


Fig. 2. Measurement periods of networks contained in ISMN (in orange). Important satellite missions providing soil moisture information and two widely used model-based soil moisture data sets are included in blue and green, respectively (status November 2012).

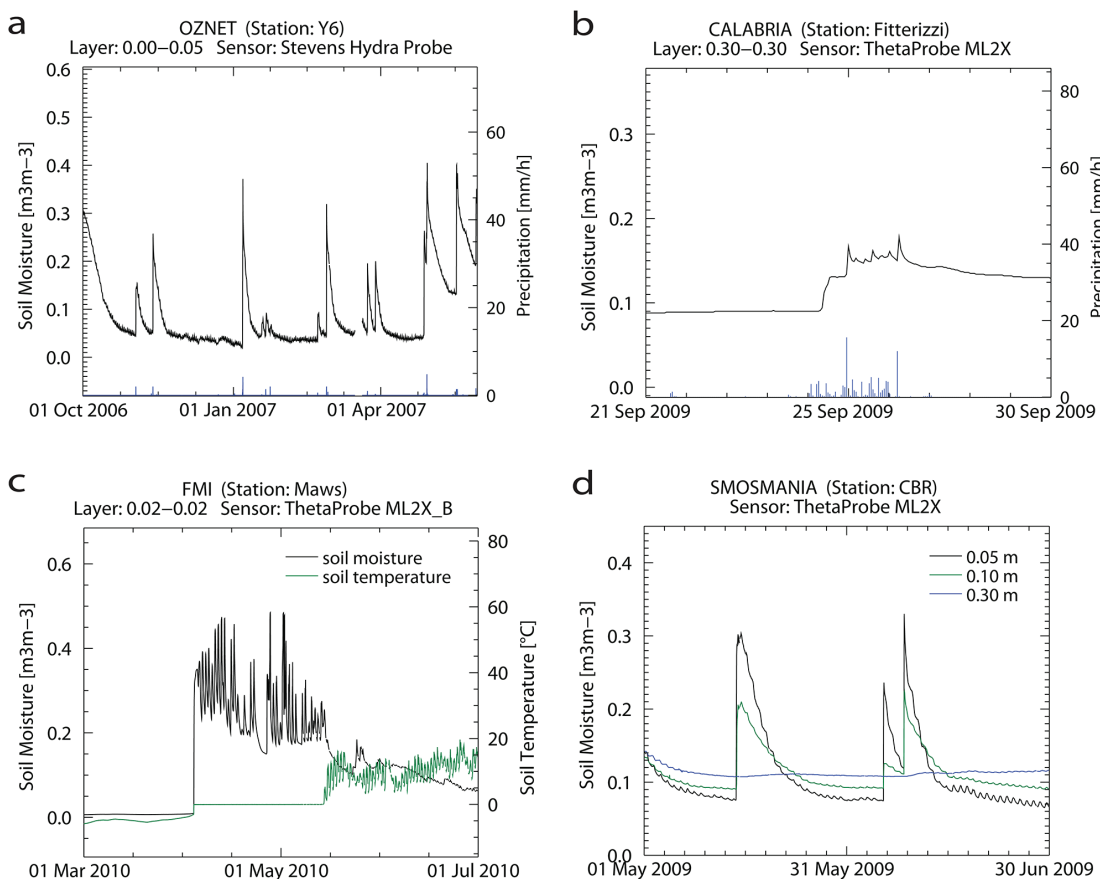


Fig. 3. (a) Example of typical soil moisture wetting and drying behavior. (b) Example of soil moisture measurements during consecutive precipitation events. (c) Example of registered soil moisture behavior in case of a frozen soil and subsequent cycles of thawing and refreezing. (d) Example of temperature sensitivity of soil moisture at different depths.

where a daily fluctuation is observed in soil moisture values, showing relatively high values in the afternoon and low values during night. Typically, such temperature-related fluctuations stay within the specifications of the manufacturer's accuracy of 0.01 to 0.05 $\text{m}^3 \text{ m}^{-3}$ (Robinson et al., 2008; Young et al., 2008). In Fig. 3d we can see that artificial diurnal soil moisture fluctuations reduce with increasing depth, which corresponds to reduced temperature fluctuations at greater depths.

Errors in In Situ Soil Moisture Readings

Random Noise and Spikes

Random noise is intrinsic to any measurement. By definition, random noise is scattered around the true value following a probability density distribution function around a null expected value, which makes it well predictable. Therefore, we do not regard it as an error but report it here for reasons of completeness. If noise is visible in the data depends on the signal/noise ratio and the radiometric precision of the sensor. Notice that noise is different from the regular daily oscillations induced by temperature fluctuations as its behavior is entirely random, and there is no inverse relationship with depth (Fig. 4a).

Spikes are different from noise as they typically last only one time step and are unpredictable with respect to their magnitude (Fig. 4b). Spikes result, for example, from temporary sensor failure or reduced current supply.

Breaks

As breaks we typify sudden increases (jumps) or decreases (drops) in the registered soil moisture value, usually from one time unit to the next. Often they result from a reduced power supply or a sudden change in the environmental conditions. Unlike spikes, jumps and drops lead to a (semi-) permanent offset of measurement values with respect to the preceding period. However, it is often difficult to establish which of the periods (i.e., before or after the event) represents the situation closest to the truth. Examples of a jump and a drop can be seen in Fig. 5.

Constant Low and High Values

Several phenomena may be responsible for the registration of a constant value over time. Frost

periods and longer sensor drop outs (Fig. 6a) commonly lead to invariable low registered soil moisture values. A constant high signal may be registered when the soil moisture content exceeds the upper limit of sensitivity of the sensor. In time series such events appear as plateaus (Fig. 6b). This behavior is often observed for capacitance probes (Mittelbach et al., 2011).

Other Sources of Error

Basara and Crawford (2000) observed a rapid wetting of deeper sensors after precipitation events. This was caused by the preferential flow through the (refilled) trench dug to install the sensors. Even though the sensors were operating properly in this case, the variations measured did not represent conditions in the surrounding soil.

Systematic differences, or biases, may exist between measured soil moisture and the true soil moisture content. They result, for example, from inappropriate calibration or a lack of representativeness of the point measurement for a larger soil volume. As the true soil moisture content is usually not known, biases are difficult to characterize. Nevertheless, they can be reduced by appropriate sensor calibration (You et al., 2010).

An instrument drift stands for a gradual systematic change over time that cannot be related to changing climatological conditions.

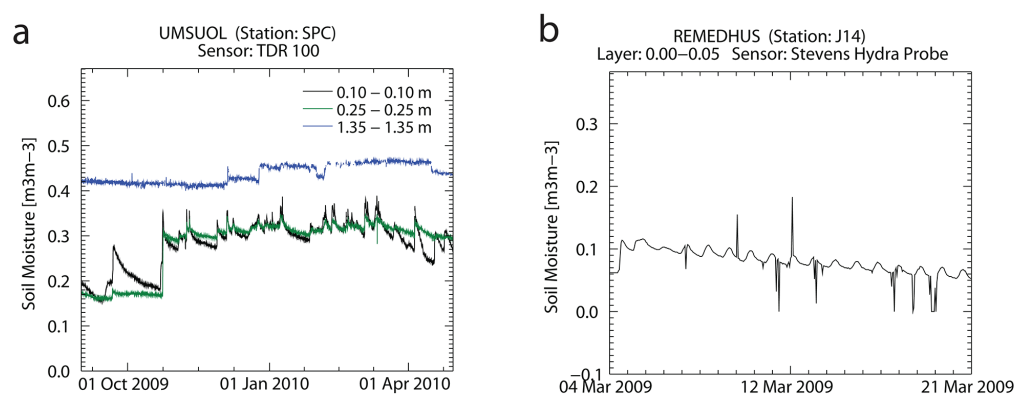


Fig. 4. Example of soil moisture measurement series containing (a) random noise and (b) spikes.

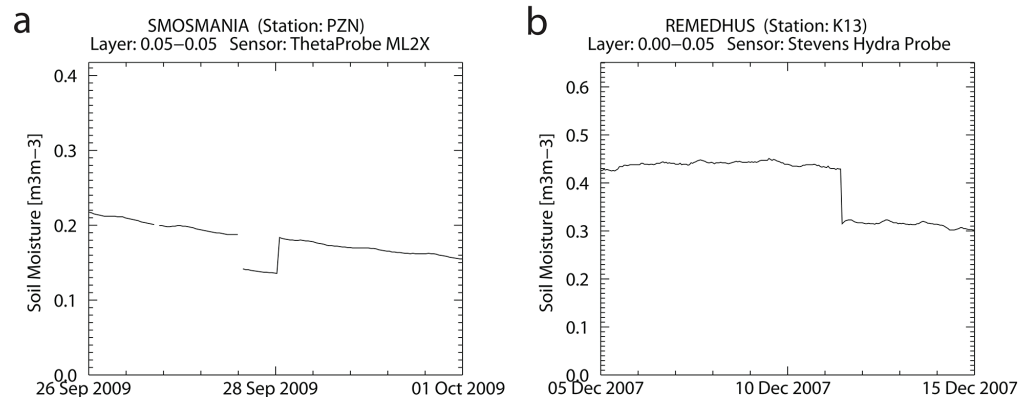


Fig. 5. Example of a soil moisture time series with (a) a jump and (b) a drop.

A sensor drift may be caused e.g., by ongoing oxidation of the sensor rods, salinization, increasing soil compaction, or changes in subsurface flow conditions. As drifts take effect over longer time periods and are difficult to separate from long-term and seasonal fluctuations, long observation periods are needed to characterize them.

Quality Control Methods

The best quality control of observational data is typically obtained through visual inspection. However, for a large volume of data and operational applications this is mostly not possible. The aim of the ISMN QC module is, therefore, to identify and flag spurious observations automatically, that is, without visually inspecting the data. The data values themselves are not manipulated (e.g., by filtering or smoothing), neither removed from the database, which allows for a further processing by the users.

Two different subsets were used to develop the methods for QC. For developing the geophysical dynamic range and geophysical consistency methods (see “Checking Geophysical Consistency” below) 10 stations from 9 different networks were selected that, in addition to soil moisture measurements, also provided measurements of soil temperature and precipitation (Table 2). A subset of 15 stations from 9 different networks (Table 3) was selected to develop spectrum-based QC algorithms that are presented in the sections “Spectrum-Based Approaches,” “Break Detection,” and “Detection of Constant Values.” Selection of these stations was based on the known occurrence of various types of errors and represents a variety of soil moisture sensors, measurement depths, and climate conditions. Independent data sets were used to validate the transferability of the methods (Tables 4 and 5). The validation data sets were carefully visually inspected and erroneous measurements were manually flagged according to the different categories of errors specified. Notice that the validation is not intended to serve as a comprehensive error assessment, but to highlight general performance of the QC and to identify potential causes of inadequate flagging.

In the following, a series of methods is proposed to identify most of the errors described in the previous

section. However, the QC system does not characterize systematic errors like biases and drifts as long measurement time series are needed to describe them in a robust way, a prerequisite that is not given for many data sets. Neither systematic noise is addressed here. Baseline of the methods proposed in this section (apart from the geophysical dynamic range tests) is an hourly sampling interval.

Checking Geophysical Dynamic Range

A threshold method is applied to detect soil moisture observations exceeding the geophysical plausibility range. This check is rather simple to implement since only the observation at time t and thresholds for the individual observation site are needed. Therefore, this test could be implemented in an NRT automated quality control procedure. Dorigo et al. (2011b) proposed several minimum and maximum thresholds for flagging the variables contained in the ISMN. For soil moisture they adopted a range of 0.0 to 0.6 $\text{m}^3 \text{m}^{-3}$, which we also use in this study.

Physically, soil moisture content is limited by the porosity of the soil (Hillel, 1998). Thus, instead of using a single global threshold, it would be more appropriate to flag values exceeding the local

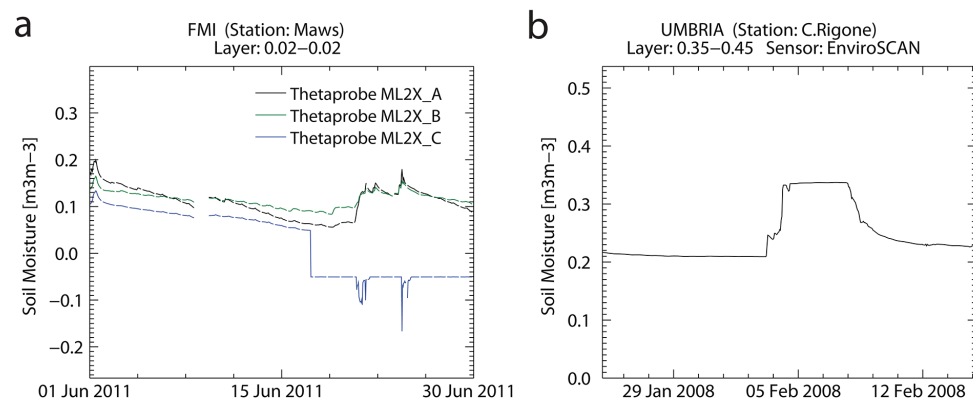


Fig. 6. (a) Stable low soil moisture value most likely caused by a sensor drop out. (b) Example of a plateau within a soil moisture time series caused by a saturated signal.

Table 2. Data sets and periods used for developing geophysical dynamic range and consistency quality control methods.

Network	Station	Sensor	Depth interval	Period
AMMA	AF	CS616_1	0.05–0.05	Jan. 2005–Dec. 2008
ARM	E10	Water Matric Potential Sensor 229L	0.05–0.05	July 1996–Oct. 2011
CALABRIA	Fitterizzi	ThetaProbe ML2X	0.30–0.30	Jan. 2001–May 2010
FMI	Maws	ThetaProbe ML2X_A	0.02–0.02	Jan. 2007–Dec. 2011
OZNET	M4	CS615	0.00–0.08	Sept. 2001–May 2011
OZNET	Y7	CS616	0.00–0.30	Dec. 2003–May 2011
REMEDHUS	F06	Stevens Hydra Probe	0.00–0.05	Mar. 2005–Dec. 2011
SCAN	2039	Hydaprobe Analog (2.5 V)	0.05–0.05	June 2000–Dec. 2011
UMBRIA	C.Belfiore	EnviroSCAN	0.05–0.15	Apr. 2007–May 2008
USDA-ARS	WG	Hydaprobe Analog (2.5 V)	0.00–0.05	June 2002–July 2009

Table 3. Data sets and periods used for developing spectrum-based quality control methods.

Network	Station	Sensor	Depth interval	Period	Error types
m					
FMI	Maws	Theta Probe ML2X	0.02–0.02	May 2011–July 2011	negative breaks, low level plateau
REMEDHUS	H13	Stevens Hydra Probe	0.00–0.05	July 2010–Dec. 2011	none
REMEDHUS	J14	Stevens Hydra Probe	0.00–0.05	Feb. 2009–Apr. 2009	spikes
OzNet	K11	Stevens Hydra Probe	0.00–0.05	Dec. 2006–Feb. 2007	breaks
SCAN	2052	Hydra Probe Analog	0.51–0.51	July 2008–Nov. 2009	noisy data
SCAN	2054	Hydra Probe Analog	1.02–1.02	Feb. 2002– May 2012	saturation plateaus
SCAN	2075	Hydra Probe Analog	0.20–0.20	May 2010–Nov. 2010	spike
SMOSMANIA	PZN	ThetaProbe ML2x	0.10–0.10	June 2009–July 2009	breaks
SMOSMANIA	SVN	ThetaProbe ML2X	0.10–0.10	May 2010–Dec. 2010	saturated plateaus, breaks, noisy data
SWEX_POLAND	P2	D-LOG-mpts_D	0.10–0.10	Nov. 2008–Dec. 2008	breaks, noisy data
SWEX_POLAND	P3	D-LOG-mpts_C	0.10–0.10	Aug. 2009–Sept. 2009	breaks, spikes
UDC_SMOS	80	EC5 II	0.05–0.05	May 2009–Mar. 2010	missing values, spikes, breaks
UDC_SMOS	501	EC5 I	0.05–0.05	Dec. 2010–Apr. 2011	saturation plateaus
UMBRIA	C.Rigone	EnviroSCAN	0.15–0.25	Apr. 2008–May 2008	saturation plateaus
USDA-ARS	WG	Hydraprobe Analog (2.5 V)	0.00–0.05	Sept. 2006–Jan. 2008	breaks, low level plateaus, spikes

saturation point or porosity. Besides the fact that porosity measurements are prone to large measurement uncertainties, they are mostly not determined at the locations of the installed sensors. Therefore we propose to calculate soil porosity from soil texture and organic carbon contents as provided by Harmonized World Soil Database (HWSD) (FAO/IIASA/ISRIC/ISS-CAS/JRC, 2009), which at present is assumed to be the most consistent soil database at a global scale. Based on the soil parameters, soil porosity is calculated using the pedotransfer equations of Saxton and Rawls (2006).

Table 4. Data sets used for evaluating geophysical dynamic range and consistency quality control methods.

Network	Station	Sensor	Depth interval	Period
m				
ARM	E24	Water Matric Potential Sensor 229L	0.05–0.05	Feb. 2000–Nov. 2009
HYDROL-NET	WEEF	TDR- TRASE-BE	0.05–0.05	Jan. 2010–Dec. 2010
MOL-RAO	GM	TRIME-EZ	0.08–0.08	Jan. 2003–Dec. 2008
OZNET	K6	Stevens Hydra Probe	0–0.05	Nov. 2003–May 2011
OZNET	M6	CS615	0–0.08	Sept. 2001–May 2011
SCAN	2119	Hydraprobe Analog	0.05–0.05	May 2010–Dec. 2011
SCAN	2141	Hydraprobe Digital Sdi-12	0.05–0.05	Oct. 2007–Dec. 2011
SCAN	2047	Hydraprobe Analog	0.05–0.05	Feb. 2010–Dec. 2011
SCAN	3024	Hydraprobe Digital Sdi-12	0.05–0.05	June 2011–Dec. 2011
SNOTEL	979	Hydraprobe Analog	0.05–0.05	Oct. 2001–Dec. 2011
SNOTEL	1030	Hydraprobe Analog	0.05–0.05	Jan. 2005–Dec. 2011

Checking Geophysical Consistency

To check the geophysical consistency of soil moisture measurements they can be confronted with other closely related variables describing the land–atmosphere system. These variables can be measured at the same location or extracted from additional observation- or model-based global data sets. In Dorigo et al. (2011b) several plausibility checks were introduced based on soil and air temperature and precipitation measured in situ. Since these auxiliary variables are not provided for all stations as in situ measurements, this study extends and improves the geophysical plausibility check using external data sets. Consistency checks against other geophysical parameters can only be performed in

NRT if the corresponding data sets are available within 3 h of sensing as well. Consequently, NRT requirements pose a strong constraint on operational QC.

Using Precipitation

The relation between precipitation and soil moisture response has already been proposed as a basis to identify spurious soil moisture observations. For instance, You et al. (2010) proposed a simplified water balance model based on precipitation and irrigation amount. However, their method led to significant overflagging. Dorigo et al. (2011b) proposed to flag constant or decreasing soil moisture levels in combination with a precipitation event measured in situ.

Table 5. Data sets and periods used for evaluating spectrum-based quality control methods.

Network	Station	Sensor	Depth interval	Period	Error types
m					
AMMA	TK	CS616	0.05–0.05	Jan. 2006–Dec. 2009	breaks, SM† below 0
AMMA	WK	CS616	1.00–1.30	Jan. 2006–Dec. 2009	none
AMMA	NT	CS616	1.00–1.00	Jan. 2006–Dec. 2009	saturated plateaus
AMMA	AF	CS616	0.60–0.60	Jan. 2005–Dec. 2008	SM below 0
AMMA	AF	CS616	1.20–1.20	Jan. 2005–Dec. 2008	SM below 0
ARM	M1	SMP1	0.03–0.03	Oct. 2010–Apr. 2011	saturated plateaus
CALABRIA	Chiaravalle	ThetaProbe ML2X	0.30–0.30	Jan. 2001–May 2010	breaks, low level plateau
CAMPANIA	Melizzano	ThetaProbe ML2	0.30–0.30	July 2000–Dec. 2008	saturated plateau
FMI	Maws	ThetaProbe ML2X	0.02–0.02	Jan. 2007–May 2012	SM below 0
FMI	Maws	ThetaProbe ML2X	0.02–0.02	Jan. 2007–May 2012	SM below 0
HSC-SELMACHEON	Selmacheon	Hydraprobe Analog (CR800)	0.00–0.10	Jan. 2008–Jan. 2009	breaks
HYDROL-NET	WEEF	TDR	0.15–0.15	Jan. 2010–Dec. 2012	none
IIT_KANPUR	IITK_Airstrip	Water Scout SM100	0.50–0.50	June 2011–Dec. 2011	none
MAQU	CST_03	ECH20 EC-TM	0.05–0.05	July 2008–July 2010	noisy data
METEROBS	Monte Pino	EnviroSCAN	0.20–0.20	Oct. 2011–Mar. 2012	none
MOL-RAO	GM	TRIME-EZ	0.90–0.90	Dec. 2002–Dec. 2008	(negative) spikes
OZNET	A4	CS615	0.00–0.08	Nov. 2001–May 2011	no rain but rise in SM
OZNET	K5	CS615	0.60–0.90	Nov. 2001–Dec. 2012	none
OZNET	M1	CS615	0.00–0.08	Sept. 2001–May 2011	none
OZNET	M6	CS615	0.00–0.08	Sept. 2001–May 2011	none
OZNET	Y5	Stevens Hydra Probe	0.00–0.05	Dec. 2003–May 2011	no rain but rise in SM
REMEDHUS	H11	Stevens Hydra Probe	0.00–0.05	Mar. 2005–May 2007	none
SASMAS	G1	Stevens Hydra Probe	0.00–0.30	Dec. 2005–Dec. 2007	none
SCAN	2085	Hydraprobe Analog	0.05–0.05	Feb. 2004–May 2012	no rain but rise in SM
SCAN	2094	Hydraprobe Analog	0.05–0.05	June 2004–May 2012	saturated plateaus
SCAN	2171	Hydraprobe Digital sdi-12	0.05–0.05	Mar. 2010–May 2012	no rain but rise in SM
SMOSMANIA	BRN	ThetaProbe ML2X	0.30–0.30	Jan. 2009–Jan. 2011	SM > 0.6
SMOSMANIA	PZN	ThetaProbe ML2X	0.05–0.05	Jan. 2009–Jan. 2011	breaks
SNOTEL	349	Hydraprobe Analog	0.20–0.20	July 2007–May 2012	periods with SM = 0
SNOTEL	957	NS	0.05–0.05	Aug. 2007–May 2012	spikes, breaks, low plateau, SM > 0.6, noise
SWEX_POLAND	Bubnow-Polesie	D-LOG-mpts	0.30–0.30	Aug. 2006–Sept. 2009	spikes, breaks, saturated plateaus
SWEX_POLAND	P3	D-LOG-mpts	0.10–0.10	Dec. 2008–Jan. 2012	spikes, breaks, SM > 0.6
UDC_SMOS	16	IMKO TDR	0.20–0.20	Mar. 2008–Nov. 2011	noisy data
UDC_SMOS	49	IMKO TDR	0.00–0.10	Mar. 2008–Nov. 2011	SM > 0.6
UDC_SMOS	80	EC5 III	0.05–0.05	Mar. 2008–Mar. 2010	spike (below zero)
UDC_SMOS	501	EC-ET 2	0.05–0.05	Apr. 2010–Oct. 2011	saturated plateaus
UMBRIA	C.Belfiore	EnviroSCAN	0.15–0.25	Apr. 2007–May 2008	none
UMBRIA	C.Rigone	EnviroSCAN	0.35–0.45	Apr. 2007–May 2008	saturated plateau
UMSUOL	SPC	TDR 100	0.25–0.25	June 2009–Sept. 2010	spikes, noisy data
UMSUOL	SPC	TDR 100	0.45–0.45	June 2009–Sept. 2010	noisy data
UMSUOL	SPC	TDR 100	1.80–1.80	June 2009–Sept. 2010	noisy data
USDA-ARS	WG	Hydraprobe Analog	0.00–0.05	June 2002–July 2009	breaks, low level plateaus, spikes
VAS	Melbex_I	Stevens Hydraprobe	0.00–0.05	Jan. 2010–Jan. 2012	none

† Soil moisture.

In our study, we refine the check proposed by Dorigo et al. (2011b) by flagging an observation as questionable if there is a rise in soil moisture but no significant rainfall amount in the preceding 24 h. To generalize the method for stations where no in situ precipitation measurements are available, we propose using GLDAS-Noah precipitation data (Rodell et al., 2004), which has been shown to provide reliable estimates of precipitation in mid-latitudes (Wang et al., 2011). GLDAS precipitation data is based on the NOAA Climate Prediction Center's operation global 2.5° 5-d Merged Analysis of Precipitation (CMAP), which is a blending of satellite (IR and microwave) and gauge observations. Global Data Assimilation System (GDAS) (Derber et al., 1991) modeled precipitation is used to disaggregate the CMAP fields spatially and temporally to match the GLDAS resolutions. GLDAS-Noah precipitation data ($\text{kg m}^{-2} \text{S}^{-1}$) are available at a 3-h temporal resolution and converted to millimeters per hour. From 2000 onward the spatial resolution is 0.25° ; for the period 1979–1999 data are available at a reduced resolution of 1.0° .

Significant rises in soil moisture (i.e., those exceeding temperature-induced daily variations and noise) are identified if the following conditions at time step t apply:

$$x_t > x_{t-1} \quad [1]$$

$$x_t - x_{t-24} > 2\sigma_{x[t-24,t]} \quad [2]$$

where x_t is the soil moisture value at timestep t in hours and $\sigma_{x[t-24,t]}$ the standard deviation of x over the preceding 24 h. The first condition ensures that only rises in soil moisture are flagged. The second condition ensures that the identified rise in soil moisture exceeds the daily variation in soil moisture, e.g., induced by temperature fluctuations.

For each measurement identified as a rise in soil moisture according to Eq. [1] and [2] we check the occurrence and amount of precipitation in the 24 h before the measurement. If a rise in soil moisture but no precipitation is identified during the preceding 24 h, the measurement is flagged. If a precipitation event is actually detected by the soil moisture sensor depends on the amount of precipitation, the installation depth of the sensor, and the accuracy of the sensor. Therefore, the minimum amount of precipitation (in m) needed for a sensor response is given by:

$$P_{\min} = DA_p \quad [3]$$

where D is the measurement depth of the sensor (m), A the accuracy of the sensor, and p the soil porosity. Here we use an average sensor accuracy of $0.05 \text{ m}^3 \text{ m}^{-3}$, and an average p of 0.5. If the total precipitation in the previous 24 h of a soil moisture measurement (P) is less than P_{\min} , the soil moisture measurement is flagged.

The precipitation-based method is only applied to surface soil moisture measurements (<10 cm), which show a direct response to precipitation. First, the method for detecting a rise in soil moisture is tested using 10 visually controlled reference stations. Next, we compare the flagging results based on GLDAS-Noah with those obtained using in situ precipitation data to quantify the effectiveness of using a global precipitation product.

Using Soil Temperature

Dorigo et al. (2011b) proposed the use of in situ soil temperature measurements to detect spurious soil moisture observations due to frost. To make this method universally applicable we tested the use of GLDAS-Noah soil temperature data for this purpose (Rodell et al., 2004). GLDAS-Noah soil temperature data are available every 3 h at a spatial resolution of 0.25° (2000–present) and 1.0° (before 2000). Soil moisture values are flagged if the modeled soil temperature drops below 0°C . To quantify the capability of coarse resolution GLDAS-Noah in capturing spurious soil moisture observations the results are compared to the results obtained using soil temperature data measured in situ.

Spectrum-Based Approaches Spike Detection

As shown in Fig. 3a, rainfall events lead to a crisp rise in soil moisture content while the drying process occurs at a slower rate following an almost asymptotic shape. Traditional spike detection algorithms like presented in DATA-MEQ (2010) have been designed for data types that naturally exhibit smoother temporal behavior. Accordingly, they tag precipitation-induced sudden rises in soil moisture as erroneous. Therefore, we introduce a new spike detection method based on a series of conditions applied to the measured moisture values and their second derivatives. The derivatives were calculated using a Savitzky–Golay filter with a window size of 3 h and a second-order polynomial fit (Savitzky and Golay, 1964).

Only if there is a substantial change in soil moisture between two consecutive time steps, that is, a minimum increase or decrease of 15% (which is three times the maximum sensor uncertainty) compared to the previous value, the reference time step t is identified as potential spike:

$$\frac{x_t}{x_{t-1}} > 1.15$$

or

$$\frac{x_t}{x_{t-1}} < 0.85 \quad [4]$$

Since Eq. [4] is not able to distinguish a spike from a precipitation event, a second condition is added based on the typical behavior of the second derivative (x'') around a spike. A positive (negative) spike results in a strong negative (positive) peak of the second

derivative at time t surrounded by two lower positive (negative) peaks at $t - 1$ and $t + 1$. Assuming that the soil moisture content does not dramatically change between $t - 1$ and $t + 1$ the ratio between these time steps is close to unity (both for positive and negative spikes). Based on the calibration data sets it was observed that the natural variation of this ratio varies between 0.8 and 1.2:

$$0.8 < \left| \frac{x''_{t-1}}{x''_{t+1}} \right| < 1.2 \quad [5]$$

As the second derivative criterion does not work well for noisy data, we added a third criterion based on the coefficient of variation over an interval of 24 h centered at t but excluding t itself:

$$\left| \frac{\sigma^2(x_{t-12}, x_{t+12})}{\mu(x_{t-12}, x_{t+12})} \right| < 1 \quad [6]$$

where σ^2 is the variance and μ the average over the interval x_{t-12} , x_{t+12} . The threshold results from the properties of the coefficient of variation, where a value above 1 symbolizes very noisy data. An observation is flagged as a spike only if all three conditions (Eq. [4–6]) are fulfilled. It has to be noted that this check cannot be performed in NRT since a 24-h time window covering observations “from the future” is needed.

Break Detection

As for spikes, breaks are characterized by a sudden rise (jump) or decrease (drop) in soil moisture, respectively. However, while after spikes soil moisture levels steadily return approximately to their initial value, jumps and drops typically lead to an enduring offset with regard to the preceding period. The break detection algorithm presented here captures this typical behavior by looking at the time series and its first and second derivatives, which were calculated in a similar way as for the spike detection. To be flagged as a break, an observation needs to fulfill three criteria.

1. The relative change of soil moisture needs to be at least 10%. Moreover, to prevent overflagging of low absolute moisture values, the absolute change in soil moisture needs to be at least $0.01 \text{ m}^3 \text{ m}^{-3}$, leading to:

$$\frac{x_t - x_{t-1}}{x_t} < 0.1$$

and

$$|x_t - x_{t-1}| > 0.01 \quad [7]$$

2. First derivative criterion: A negative (positive) break is expressed by a strong negative (positive) change of the first derivative x'_t . Here we assume that the value shall at least be 10 times smaller (larger). To make this criterion more robust, we compare the first derivative with the average of all first derivative values within a 24-h period centered at t , leading to:

$$x'_t > 10 \frac{1}{n} \sum_{k=-12}^{12} x'_{t+k} \quad [8]$$

3. Second derivative criterion: A negative (positive) break results in a large negative (positive) second derivative at t followed by a large positive (negative) value at $t + 1$: The peaks in the second derivative are approximately of the same size (though opposite in sign) resulting in a ratio around one. At $t + 2$ the second derivative returns to a value close to zero; hence, the ratio of the absolute second derivative between at $t + 1$ and $t + 2$ is very large. This results in the following conditions:

$$\left\| \frac{x''_t}{x''_{t+1}} \right\| = 1$$

and

$$\left| \frac{x''_{t+1}}{x''_{t+2}} \right| > 10 \quad [9]$$

As no reliable statement about the plausibility of the measurements before and after the jump is possible, only the jump itself is flagged. Again, this check cannot be applied in NRT.

Detection of Constant Values

Invariant high soil moisture values (or plateaus) are identified through three conditions. First, to distinguish them from regular wetting events and spikes, the values need to remain constant for at least 12 h. Thus, for the whole data period intervals with a minimum size of 12 h are searched for which soil moisture variance shall not exceed 1% of the average sensor uncertainty of $0.05 \text{ m}^3 \text{ m}^{-3}$ (Eq. [10]). We decided to allow this small variability because soil moisture readings of plateaus are not always perfectly stable (Fig. 6a).

$$\text{interval} = [t - n, t + n]$$

while

$$\sigma^2[x_{t-n}, x_{t+n}] \leq 0.0005$$

and

$$n \geq 6 \quad [10]$$

To separate plateaus from other constant soil moisture values (e.g., after a long period without precipitation) a second criterion based on the first derivative was introduced. As plateaus typically occur after intense precipitation events, a plateau is preceded by a local maximum in the first derivative (Eq. [11]). The end of the plateau is indicated by a local minimum in the first derivative (Eq. [12]). The intervals resulting from the first conditions (Eq. [10]) serve as a basis for the examination of the local extreme values which have to meet these threshold values. Minimum and maximum threshold values of the first derivative were established from the calibration data set.

$$t = t_{\text{plateau_start}} \Leftrightarrow \exists \max([x'_{t-n-12}, x'_{t-n+12}]) \geq 0.0025 \quad [11]$$

$$t = t_{\text{plateau_end}} \Leftrightarrow \exists \min([x'_{t-n-12}, x'_{t-n+12}]) \leq 0 \quad [12]$$

Physically, plateaus always occur at the highest soil moisture values of a time series. Therefore, we added a third condition (Eq. [13]) where we assume that plateaus only occur at a soil moisture level of at least 95% of the maximum value measured during the whole observation period:

$$\mu(x_{[t_{\text{plateau_start}}, t_{\text{plateau_end}}]}) > \max(x_{t_0, t_{\text{end}}}) 0.95 \quad [13]$$

Low constant values are different in nature from plateaus as they are typically the result of frozen soils or sensor failure. While frost events can be captured by negative soil temperatures (see “Using Soil Temperature”), low-level plateaus resulting from sensor failure are preceded by a sharp negative break (Fig. 5). Hence, the negative jump detection algorithms described in “Break Detection” are first used to identify the potential offset of a low constant value. Starting from this offset, all following measurements are flagged as “low constant value” as long as they comply with:

$$\left| \frac{\sigma^2(x_t, x_{t+n})}{\mu(x_t, x_{t+n})} \right| < 0.01 \quad [14]$$

where t represents the already detected negative break and n has a minimum length of 12, in accordance with the plateaus.

Results and Discussion

Validation Based on Test Data Sets

Overall Accuracy

A classical error matrix was used to assess the performance of the flagging methods (Congalton and Green 2009; Hubbard et al., 2005). Table 6 summarizes the performance for all validation data sets listed in “Data Description.” It shows that only very low percentages of correct observations are flagged as “erroneous” while detection accuracy of erroneous observations varies between 52.2 and 97.4%. Potential causes of failing flagging procedures will be discussed in the following paragraphs. Notice that for the geophysical dynamic range and in situ-based approaches no “true” reference could be established.

Geophysical Dynamic Range

Only few observations were flagged based on threshold methods. Figure 7 shows two examples of soil moisture values exceeding the range 0.0 to $0.6 \text{ m}^3 \text{ m}^{-3}$. The first example is an obvious case of sensor failure. In the second example soil moisture values exceeding the $0.6 \text{ m}^3 \text{ m}^{-3}$ threshold are flagged though the values themselves look realistic. A possible reason for this could be a deficient calibration (multiplicative bias) or specific site conditions. More observations (about 1.5%) exceeded the saturation point, as porosity is typically lower than $0.6 \text{ m}^3 \text{ m}^{-3}$.

Unfortunately, in situ porosity was not measured for any of the validation data sets. Therefore, to obtain an indication of the plausibility of this flagging method we compared the HWSD-based and in situ-based saturation point flagging for all sites at ICN, the only network for which in situ porosity measurements are available (Table 7). There is a remarkable correspondence between the two results. Even though we expect that the use of the HSWD in

Table 6. Summary of the flagging performance based on evaluation data sets 2.

Flagging result	Erroneous measurement		Correct measurement		Flagged observations
	“Erroneous”	“Correct”	“Erroneous”	“Correct”	
Soil moisture below $0 \text{ m}^3 \text{ m}^{-3}$	NA†	NA	NA	NA	0.0
Soil moisture above $0.60 \text{ m}^3 \text{ m}^{-3}$	NA	NA	NA	NA	0.5
Soil moisture above saturation point (based on HWSD)	NA	NA	NA	NA	1.5
Soil moisture in combination with negative soil or air temperature (in situ)‡	NA	NA	NA	NA	4.5
Soil moisture in combination with negative soil temperature (GLDAS-Noah)	92.6	7.4	9.8	90.3	14.4
Precipitation in combination with equal or decreasing soil moisture‡	NA	NA	NA	NA	3.3
Precipitation-based flagging (GLDAS)	63.1	36.9	2.2	97.8	2.4
Spikes	80.0	20.0	0.2	99.8	0.04
Positive breaks (jumps)	52.2	47.8	0.0	100.0	0.01
negative breaks (drops)	71.8	28.2	0.0	100.0	0.01
Constant values following negative break	97.4	2.6	0.1	99.9	0.07
Plateaus	76.2	23.8	1.5	98.5	2.83

† NA, not applicable.

‡ After Dorigo et al. (2011a).

combination with the pedotransfer functions will not provide such good results for all stations (e.g., for peat soils), the large-scale data set seems to have high potential for local purposes.

Geophysical Consistency

Flagging spurious observations based on negative soil temperature is very straightforward and mainly depends on the quality of the soil temperature data set used. The use of GLDAS-Noah soil temperatures was very successful, as it was able to flag 92.6% of the observations that were flagged as spurious based on in situ soil temperature data.

Figure 8 shows an example of flagging soil moisture measurements based on negative soil temperature from GLDAS-Noah and in situ data, respectively. In both cases flagging looks appropriate, given the sudden sharp decrease in soil moisture content. The plot also shows that not all spurious observations were flagged, neither using the GLDAS data (end of freezing event remains unflagged), nor using the in situ data (onset of event is missed). Overall, GLDAS-Noah flagged a considerably higher percentage (14.4%) of observations compared to the use of in situ air and soil temperatures as proposed by Dorigo et al. (2011b) (Table 6).

Flagging rises in soil moisture that cannot be related to precipitation events are a more intricate question, as the result depends both on the success of the automated method to detect rises in soil moisture and, once rises have been identified, the capability of a global precipitation data set in flagging spurious observations. First, we assessed the capability of Eq. [2] to detect rises in soil moisture by comparing the results with visually checked rises in soil moisture based on the validation data set. 90.2% of the rises in soil moisture identified by the visually checked validation data set were also identified by the automated method. Even though the threshold used in Eq. [2] to separate events from non-events may look somewhat arbitrary, it constitutes a balanced trade-off between correctly identifying as many real rises as possible while not flagging other variations in the measured soil moisture signal (Table 8, Fig. 9). As can be seen in both the table and the figure a tighter threshold would lead to significant underflagging while a less conservative decision rule would also flag artifacts like the daily variations. The soil moisture rise detection method encounters difficulties when data are noisy or subject to freeze-thaw induced variations in measured soil moisture. In periods with several consecutive precipitation events the automated detection method is incapable of discerning all individual rises.

Second, we tested the effect of using a global precipitation data set instead of precipitation measured in situ based on the visually identified rises in soil moisture described earlier. 74.1% of the data flagged using in situ precipitation

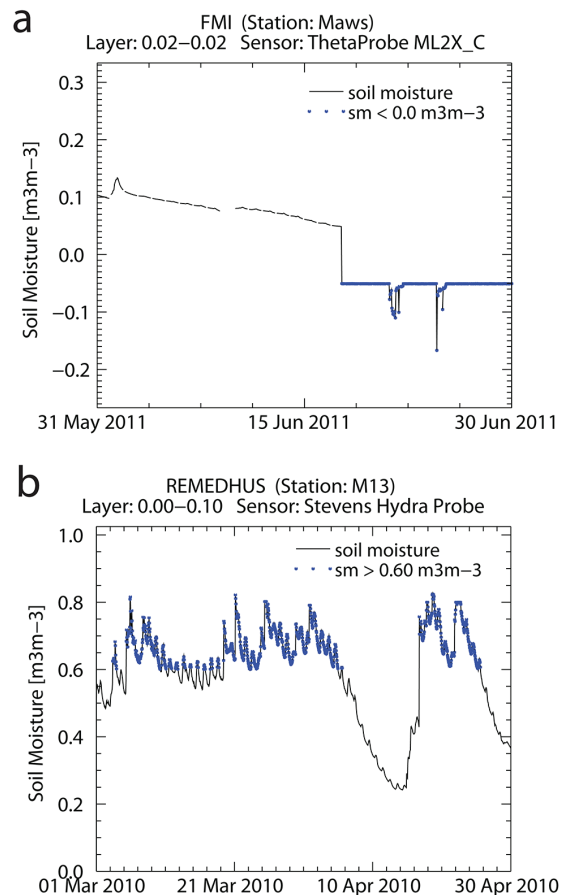


Fig. 7. Examples of flagged soil moisture measurements (blue dots) (a) below or (b) above the plausible geophysical dynamic range of 0 to $0.60 \text{ m}^3 \text{ m}^{-3}$.

data were also detected by the same procedure but using GLDAS-Noah precipitation data. This is an encouraging result, given the large discrepancy in spatial scales. Moreover, one should also take into account the uncertainty of the in situ precipitation measurements. This is illustrated in Fig. 10, which shows two examples of precipitation-based flagging using GLDAS-Noah precipitation estimates versus precipitation measured in situ. Figure 10b shows several measurements that are flagged using in situ precipitation data, while they are not being flagged using the GLDAS data (Fig. 10a). However, the soil moisture time series show a typical wetting and consecutive drying of the soil associated to precipitation events (i.e., flagging these values as spurious would be incorrect). This means that in this case the GLDAS-Noah data set provides a more reliable estimate of precipitation than the in situ measurements. The impact

Table 7. Correspondence between Harmonized World Soil Database (HWSD)-based and in situ-based saturation point flagging for ICN network. Here it is assumed that the flagging based on in situ porosity values represents the truth. Number of stations = 19, total number of observations = 42,279,338.

Flagging based on in situ porosity	"Erroneous"		"Correct"		Flagged observations %
Flagging based on HWSD porosity	"Erroneous"	"Correct"	"Erroneous"	"Correct"	
Soil moisture below $0 \text{ m}^3 \text{ m}^{-3}$	98.8	1.2	0.3	99.7	0.3

of a malfunctioning precipitation sensor becomes obvious in Fig. 10d where many events are being falsely flagged in the in situ data while no flagging occurs based on GLDAS precipitation.

Finally, the combination of the rise in soil moisture detection method and the use of a global precipitation data set results in a combined accuracy of 63.1% to correctly detect erroneous measurements with respect to visually checked events and in situ precipitation. It is expected that some improvement can still be achieved by using a precipitation product that resolves rainfall at a finer spatial scale. This may lead to an improvement especially for areas dominated by fine scale convective precipitation, such as the tropics. In these areas most state-of-the-art coarse-scale models show large uncertainties (Taylor et al., 2012). As a rough indication of the reliability of GLDAS precipitation for regions with different precipitation regimes, for each main Köppen–Geiger group (Peel et al., 2007) we calculated the average correspondence in occurrence between GLDAS precipitation and precipitation from all available in situ stations that measure precipitation as an additional component (Table 9). The agreement is high in tropical, (semi-)arid, and temperate regions. Only for the continental class, which also includes sub-arctic regions, the agreement is somewhat poorer. This may be related to the fact that part of the precipitation falls as snow in these areas.

The new flagging procedure flags a lower number of observations than the method currently employed in the ISMN (Table

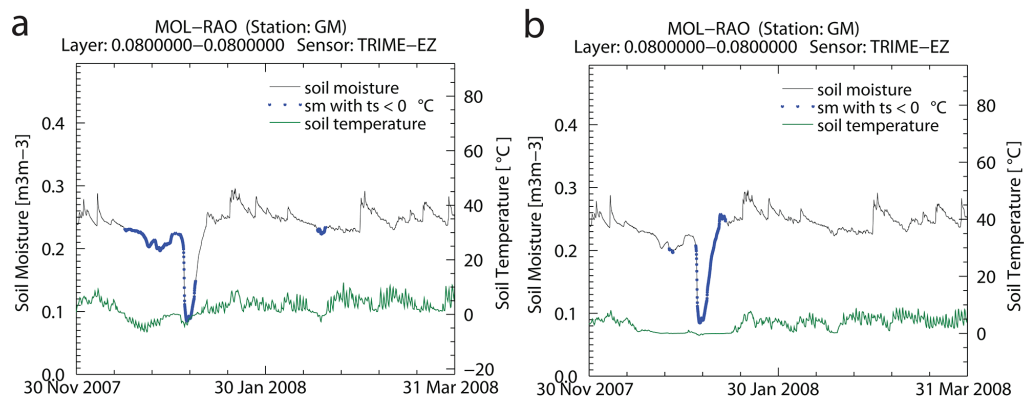


Fig. 8. Example of geophysical dynamic range flagging for soil moisture using soil temperature data either (a) from GLDAS-Noah or (b) measured in situ.

Table 8. Results of testing the rise in soil moisture detection method.

Method	Rises in soil moisture accurately detected	Stable or decreasing soil moisture accurately detected	Observations flagged as rise in soil moisture
	%		
$x_t - x_{t-24} > 4\sigma_{x[t-24,t]}$	53.3	99.7	0.5
$x_t - x_{t-24} > 3\sigma_{x[t-24,t]}$	82.3	98.4	2.6
$x_t - x_{t-24} > 2\sigma_{x[t-24,t]}$	90.2	96.2	5.3
$x_t - x_{t-24} > \sigma_{x[t-24,t]}$	92.8	93.9	7.6
$x_t - x_{t-24} > 0$	93.9	91.5	10.1

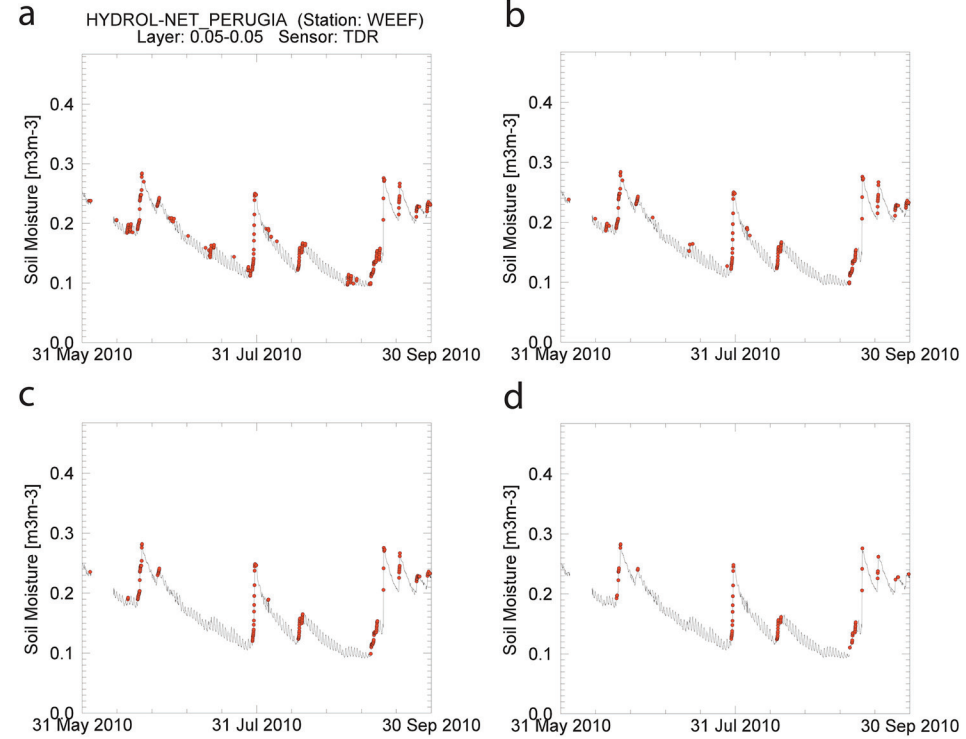


Fig. 9. Example of automated detection method for rises in soil moisture, where the minimum difference for $x_t - x_{t-24}$ is set to (a) 0, (b) to one times the standard deviation over the preceding 24 h, (c) two times the standard deviation over the preceding 24 h, and (d) three times the standard deviation over the preceding 24 h.

6). Visual inspection revealed that the existing method tends to overflag correct observations, in particular during dry-down periods and periods with precipitation when the soil is already saturated (results not shown).

Spectrum-Based Approaches

Eighty percent of the spikes in the reference data sets were detected. The spike detection method performs well for data sets with irregularly occurring isolated spikes (Fig. 11a) but has difficulties with noisy time series (Fig. 11b). The approach fails if spikes last longer than one time step or are surrounded by missing values (Fig. 11c).

Almost 71.8% of the negative breaks were correctly detected. The algorithm works well for clearly identifiable drops (Fig. 12) but leads to overflagging for time series that are strongly affected by noise. The success rate for positive breaks is lower, which is attributed to the fact that often it is difficult to discern artificial jumps from natural rises in soil moisture. Similarly as for the spike detection test, the break detection does not work when missing values precede the jump (Fig. 11a). The detection of low constant values, which is based on negative break detection, has a success rate of 97.4%. This number shows that once a negative break has been detected almost all subsequent constant values are appropriately identified.

The method appropriately flagged 76.2% of the observations making up a plateau. Figure 13 illustrates two typical situations where the flagging failed: the first plateau in the time series has a soil moisture level below 95% of the maximum value encountered in the time series while the second plateau is not flagged because it lasted less than 12 h.

Flagging Statistics for Entire ISMN

To obtain a more comprehensive picture of the errors occurring in the various data sets, the flagging procedures were applied to all ISMN stations (Table 10, Fig. 14 and 15). For the geophysical consistency checks only the surface layer measurements with a maximum starting depth of 0.10 m are analyzed; for all other flags all available depths were used. Notice, that the percentages

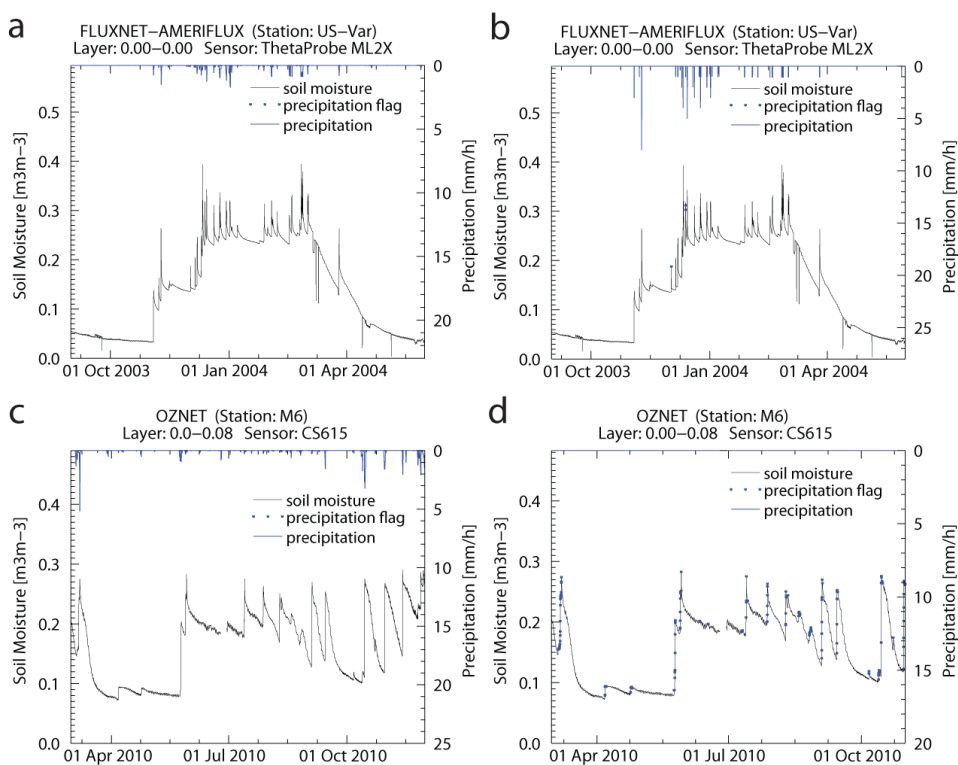


Fig. 10. Examples of geophysical consistency flagging using (a, c) GLDAS precipitation data and (b, d) in situ precipitation data. Blue dots indicate flagged observations because a rise in soil moisture is detected without a significant amount of precipitation in the preceding 24 h.

Table 9. Correspondence between precipitation occurrence in GLDAS and in situ measurements, categorized according to main level of Köppen–Geiger classification (Peel et al., 2007). Correspondence is expressed as the percentage of precipitation events measured in situ that are also visible in GLDAS data.

Group	Correspondence	Number of stations
	%	
A: tropical/megathermal climates	94.6	13
B: Dry (arid and semiarid) climates	82.5	114
C: Temperate/mesothermal climates	91.7	166
D: Continental/microthermal climate	64.1	113

per network are not corrected for the number of stations within a network (i.e., a network with many stations like SCAN has a much larger influence on the global statistics than a one-station network like UMSUOL). To facilitate calculating comprehensive statistics for all networks, only geophysical plausibility checks based on the global GLDAS-Noah data sets are shown (i.e., not the checks based on in situ data).

On average, only a low percentage of the data is flagged, which is an indicator for the generally good quality of the data. The most occurring flag is that of soil temperatures below zero. A value of 7.6% seems to be realistic given the large number of stations in areas with a pronounced cold winter season (e.g., FMI, MAQU, MONGOLIA, and SNOTEL) (Fig. 14). Since flags based on negative soil temperatures are a result of location and climatology care

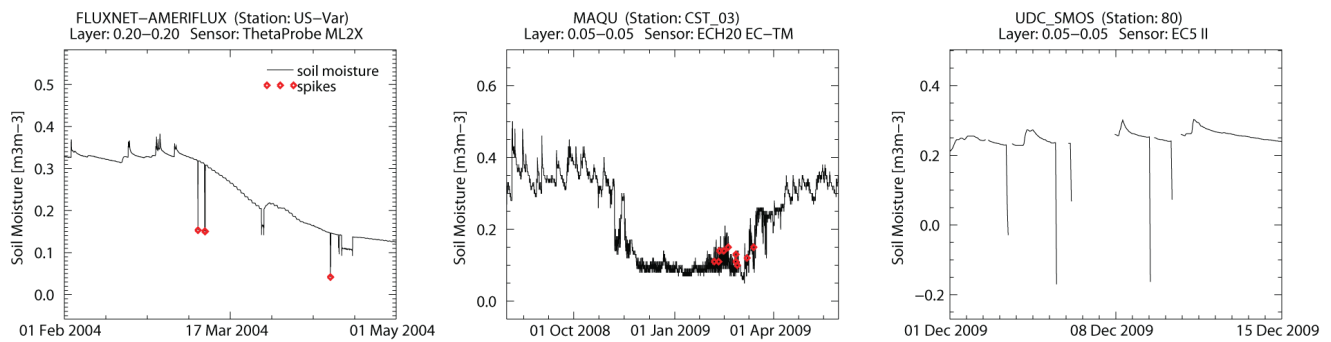


Fig. 11. Examples of spike test results.

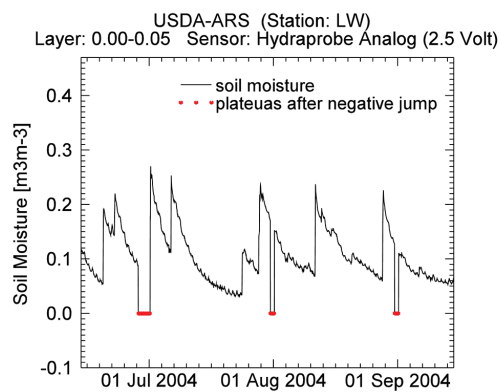


Fig. 12. Example of correctly flagged negative breaks and low constant values following these breaks.

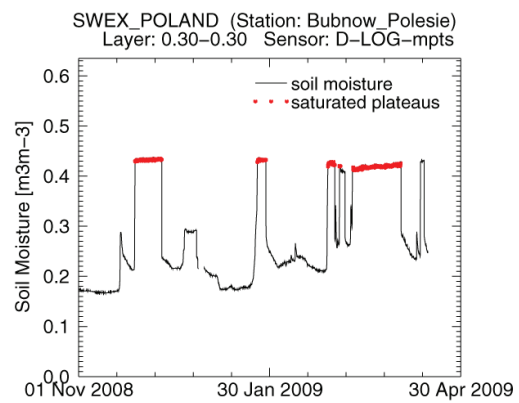


Fig. 13. Example of detected and not detected plateaus.

should be taken in using them as a relative measure of performance with respect to other stations.

The precipitation-based geophysical consistency method flagged 2.4% of the observations. Given the 63% accuracy of this flag (see “Geophysical Consistency”), the actual percentage of this type of error is expected to be approximately 1.5 times higher. Nevertheless, the precipitation-based method in our study seems to provide much more realistic values than the 10 to 27% flagged by the water balance method proposed by You et al. (2010). In their work they also concluded that their method heavily overflagged the observations.

The flag with the third largest occurrence is soil moisture above saturation point. Figure 14 shows that percentages at the network level deviate vastly with the highest percentage (37%) obtained for METEROBS. Even though the saturation point can be reliably used to filter out obvious anomalies, this flag should be carefully interpreted because it is based on a porosity map obtained from a coarse-scale soil database and may not correctly represent soil properties at the fine local scale. Still, the use of a globally available, more or less consistent data set was preferred over the use of porosity values determined *in situ* only for a very limited

Table 10. Percentages of flag occurrences based on all networks of the ISMN that provide measurements at an hourly basis.

	Flag occurrences %
Soil moisture below $0 \text{ m}^3 \text{ m}^{-3}$	0.01
Soil moisture above $0.60 \text{ m}^3 \text{ m}^{-3}$	0.16
Soil moisture above saturation point (based on HWSD)	1.19
Soil moisture in combination with negative soil temperature (GLDAS)	7.64
Rise in soil moisture without precipitation event (GLDAS)	2.42
Spikes	0.02
Negative breaks (drops)	0.01
Positive breaks (jumps)	0.01
Constant low values following negative break	0.68
Plateaus	0.67

number of stations, as the latter would lead to a quality flag that is inconsistent across the networks.

Constant values, either low values after negative breaks or plateaus, are the most frequently occurring spectrum-based flags. Figure 15 shows that percentages vary strongly from network to network.

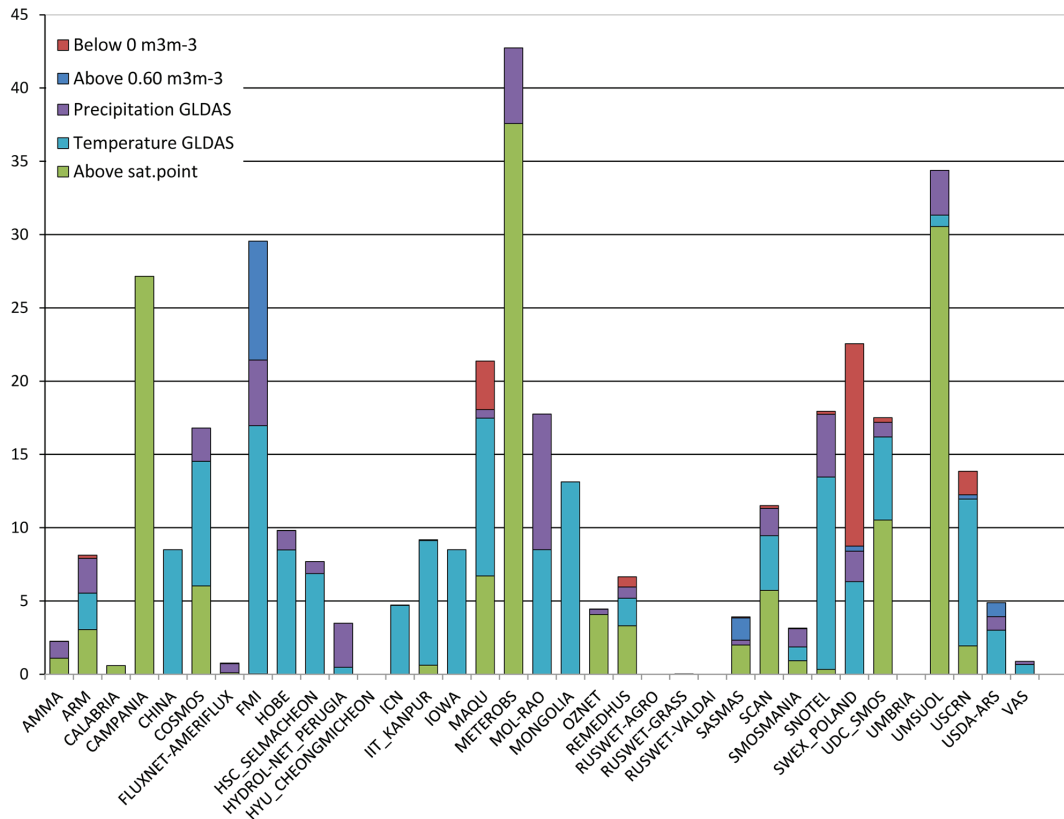


Fig. 14. Percentages of geophysical dynamic range and consistency quality flags per network.

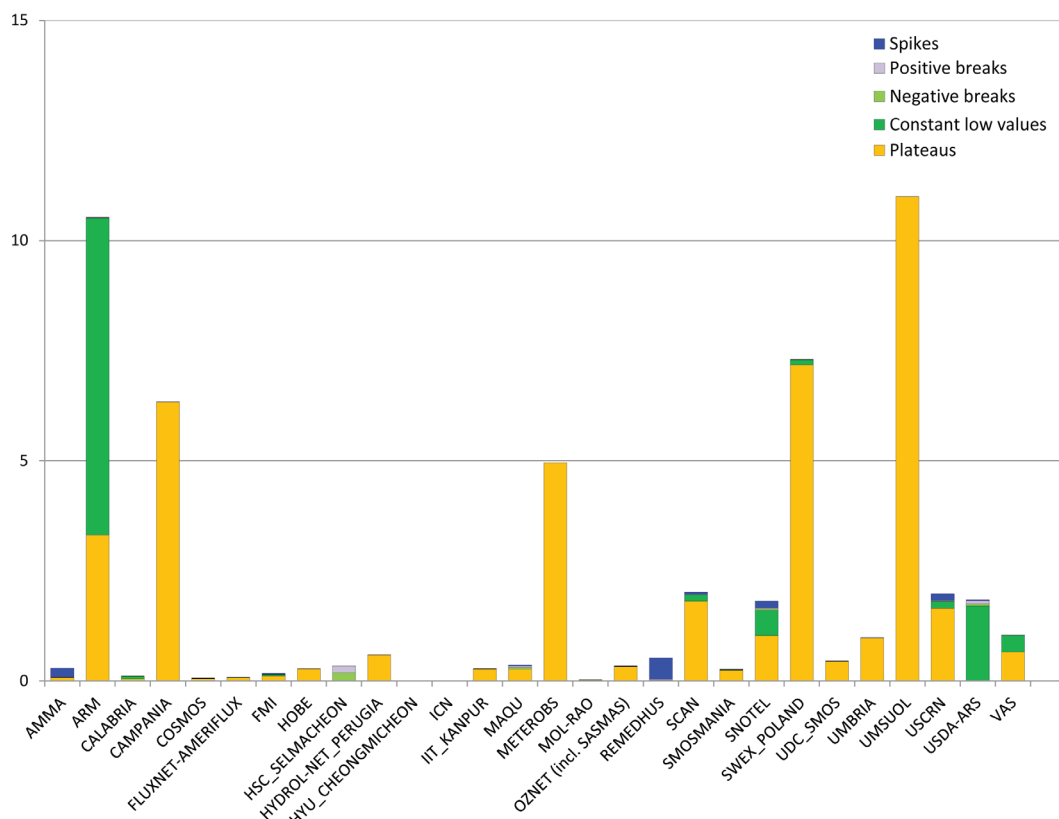


Fig. 15. Percentages of spectrum-based flags per network.

Constant low values after negative breaks are predominantly found for the ARM network. Closer inspection of the stations revealed that especially in the beginning of the measurement time series several stations were plagued by repeated sensor drop out. Other significant occurrences of constant values after negative breaks were found for the USDA-ARS, and could be confirmed by visual inspection. Repeated saturation of the sensor signal is frequently found for the ARM, CAMPANIA, SWEX_POLAND, and UMSUOL networks. The causes for this behavior can usually be well explained by physical phenomena; for example, several SWEX_POLAND stations are situated in marsh land and therefore experience continuous soil saturation, especially at deeper soil layers. Also the other networks experiencing plateaus predominantly contain sensors at deeper depths, where repeated soil saturation occurs.

Much lower percentages were found for the other flag types. Even though the number of observations flagged is lower, the number of events may be even higher than for the flag types discussed above. For example, constant values effectuate over a much longer period, and as a consequence, more observations are affected and flagged. Specifically, breaks should be studied carefully as they may lead to a permanent offset with respect to the preceding period and, hence, significantly influence validation statistics such as the root mean square error. The outlier detection results are in general agreement with the percentages obtained by You et al. (2010).

Applying the QC to all data sets in the ISMN revealed large differences in flagged values between the various networks. However, these numbers cannot be directly translated into a relative measure of performance of the networks as the data sets have undergone differing levels of QC before being submitted to the ISMN. Some of the networks were first thoroughly visually inspected while others (e.g., those provided in NRT) have not undergone any quality control at all. In addition, the number of stations contained in a network greatly determines the effect a malfunctioning sensor has on the overall network statistics. Ultimately, average network statistics are strongly influenced by the number and distribution of sensors over depth. Therefore, the flagging results should always be inspected at the level of the individual sensors before including this sensor in an envisaged analysis.

Effect on Soil Moisture Applications

To demonstrate the effect of the QC flags on potential applications, we validated the VUA-NASA AMSR-E remotely sensed soil moisture product (Owe et al., 2008) and the GLDAS-Noah modeled surface soil moisture product (0–7 cm depth; Rodell et al., 2004) for one of the ISMN sites (network SCAN, station 2110, depth = 0.05 m). Approximately one-third of the observations were flagged for this station, mainly due to observations exceeding the saturation point and $0.6 \text{ m}^3 \text{ m}^{-3}$ threshold and plateaus. Table 10 shows that in this case data flagging has a positive influence on all calculated statistical measures. The effect the flagging ultimately has

on a certain application depends on a number of factors, including the quality and representativeness of the station/sensor for the scale of the evaluated data set and the regional climate, the total number of observations flagged, and the error measure considered. For example, while the flagging of observations beyond the $0.6 \text{ m}^3 \text{ m}^{-3}$ threshold is expected to predominantly affect measures of absolute agreement (e.g., root mean square difference) the flagging of spikes is more likely to affect measures of agreement, like correlation (Table 11). It is expected that the flagging procedures will also provide a positive contribution to methodologies and studies focusing on detecting hydrometeorological extremes such as droughts and floods since some of the extremes originally encountered in the data sets can be based on artifacts (e.g., Hirschi et al., 2011).

Conclusions and Outlook

Quality control is still not a standard procedure for most networks. The aim of this study was to bridge this gap by proposing a universal and automated QC system that is applicable to the large variety of data hosted by the ISMN. The major challenge of such a system is that methods need to be transferable across networks and sensors. Therefore, the methods were either based on the shape of the measured spectrum or by using a globally available geophysical data set. It is unrealistic to assume that an automated QC system can be developed that is able to identify all spurious observations while not flagging any of the good ones (Hubbard et al., 2005). Therefore, the challenge was to find an acceptable trade-off between these two. Users commonly prefer flagging schemes where a comprehensive flagging of spurious observations is prioritized over an error-free non-flagging of good observations, as long as enough data values remain available for the analysis (Dharssi et al., 2011). However, for many soil moisture applications, such as climate research looking at trends in extremes or acceleration of the hydrological cycle (e.g., Hirschi et al., 2011), the situation is somewhat different. Too rigorous thresholds would also flag many good quality observations in the tails of the soil moisture distribution, which are of most interest to such studies. Especially rapid wetting events would be affected since confusion with spikes, positive breaks, and plateaus is high. Therefore we decided to relax somewhat the requirement of total inclusiveness in favor of preserving a representative distribution of the soil moisture values. Nonetheless, encouraging results were obtained for both error categories, especially given the heterogeneity of the networks included in the ISMN. It should also be recalled that the validation presented in this study only provides an indication of the performance and potential shortcomings of the algorithms and is by no means comprehensive. The data sets were intentionally selected for known occurrences of errors; thus, the error statistics are expected to improve further if a larger, randomly selected test data set is used.

A major trade-off of the system concerned the sampling interval of the measurements. To properly mimic the temporal dynamics we assumed that data will be available at least on an hourly basis, a

requirement that is fulfilled by all modern (semi-) automated networks. However, this has severe implications for the historical networks (CHINA, MONGOLIA, IOWA, and the RUSWET networks), where the sampling interval lies between 1 and 4 wk. Hence, for these networks only the threshold-based flagging methods make sense. Because sudden increases in soil moisture naturally occur after precipitation events it is difficult to distinguish such natural rises from abrupt breaks or spikes caused by sensor failure, even based on visual interpretation (Fig. 5). The difficulties associated with detecting natural rises in soil moisture were also reflected by the precipitation-based QC, which heavily relies on this capability. Another shortcoming of the proposed QC system concerns the inability of the system to handle large data gaps. Data interpolation methods (e.g., as proposed by Wang et al., 2012) can be considered to solve this issue, especially for smaller gaps. Other situations where the algorithms failed included the successive occurrence of multiple spikes and very noisy data.

The use of the GLDAS data sets for flagging nongeophysical values performed surprisingly well at the fine local scale of the in situ measurements. It shows that there is large potential in using global temperature and precipitation data sets. Future efforts should verify whether the use of other global data sets, such as CMORPH (Joyce et al., 2004) or ERA-Interim (Dee et al., 2011), can further improve QC based on geophysical plausibility. Also, porosity values based on the HWSD and empirical pedotransfer functions performed unexpectedly well for detecting observations exceeding the local saturation level.

The essential requirement of being generally applicable to all networks of the ISMN is at the expense of the maximum achievable accuracy, since the methods cannot be tuned for specific sensors or local conditions. Therefore, the proposed automated QC should not be considered as a replacement but rather as a complement to QC systems and expertise already existing at the side of the data providers. Feedback of local data providers having thorough knowledge on the site conditions and installation of the sensors is fundamental for understanding the potential errors identified by the automated QC system. Vice versa, network providers may benefit from this additional QC system because it may point to errors or sensor failures that have previously remained unnoticed. Therefore, future efforts will focus on integrating the QC systems existing at the network level with the one proposed in this study and to strengthen the interaction between data providers, the ISMN, and users.

Overall, the QC system provided satisfying results and is regarded a useful addition to the flags already present in the ISMN. Therefore, the new flags will soon be integrated into all existing and future data sets of the ISMN. To facilitate a proper tracking of

Table 11. Example of influence of flagging methods on soil moisture product validation (SCAN network; Station 2110, depth = 0.05 m).

		Data points	R Pearson	R Spearman	RMSE
$\text{m}^3 \text{m}^{-3}$					
AMSR-E LPRM	All data	972	0.20	0.18	0.156
	Excluding flagged data	623	0.24	0.25	0.126
GLDAS-Noah	All data	18911	0.46	0.45	0.34
	Excluding flagged data	10671	0.50	0.54	0.21

the error source, we will extend the CEOP flag definitions used to date and incorporate subcategories to describe the individual cases. The exact definition will be presented shortly on our website (<http://www.ipf.tuwien.ac.at/insitu>, accessed 28 Nov. 2012). However, we do not consider QC of the ISMN as a completed exercise. The steadily growing number of stations and auxiliary data sets pave the way for more sophisticated methods that consider the behavior of a single station with respect to that of its neighbors or an ensemble of independent data sets. Moreover, complementary methods will be exploited to characterize systematic errors of the data sets, such as biases, drifts, and random noise. The ultimate goal is to come to a comprehensive quality characterization of all stations in the ISMN, which supports users in identifying the data sets that are most appropriate for their task. Although it would be desirable to perform the automated QC in NRT or as soon as the data are being integrated in the system, we showed that the best results are obtained when auxiliary data sets and consistent time windows around individual observations were used. A regular update frequency of the flags, such as every 6 mo, instead of NRT processing is therefore envisaged.

Acknowledgments

We thank all data providers that kindly shared their data with the ISMN: Thierry Pellarin (AMMA), Jim Mather (ARM), Loredana Marsica and Luca Brocca (CALABRIA), Matteo Gentilella and Giovanni Battista Chirico (CAMPANIA), Konstantin Vinnikov and Thomas Collow (CHINA, IOWA, MONGOLIA, RUSWET-AGRO, RUSWET-GRASS, and RUSWET-VALDAI), Marek Zreda (COSMOS), Matias Takala, Hanne Suokanerva, Jouni Pullianen, Jarkko Koskinen (FMI), Alessia Flaminini and Renato Morbidelli (HYDROL-NET_PERUGIA), Simona Bircher (HOBE), Minha Choi and Yeon Gil Lee (HYU_CHEONGMICHÉON, HSC_SELMACHEON), Bob Scott (ICN), Pankaj Kumar Rai and Shivam Tripathi (ITT_KANPUR), Laura Dente, Bob Su, and J. Wen (MAQU), Nazzareno Diodato (MetEROBS), Udo Rummel (MOL-RAO), Jeffrey Walker and Christoph Rüdiger (OZNET), José Martínez Fernández (REMÉDHUS), Garry Schaeffer, Michael Strobel, Maggie Dunkle, Michael Cosh, and Robert Parry (SCAN), Jean-Christophe Calvet (SMOSMANIA), Michael Strobel and Garry Schaeffer (SNOTEL), Bogusław Usowicz, Jerzy Usowicz, and Wojciech Marczewski (SWEX_Poland), Florian Schlenz, Johanna dall'Amico, Alexander Loew, Wolfram Mauser (UDC_SMOS), Luca Brocca and Nicola Berni (UMBRIA), Vittorio Marletto and Marco Bittelli (UMSUOL), Michael Palecki (USCRN), Michael Cosh and Thomas Jackson (USDA-ARS). Without their valuable contributions this initiative would not have been possible in the first place. We thank Daniel Zamojski and Clara Cordes for helping integrate new data sets. The ISMN has been funded through the SMOS Soil Moisture Network Study (ESA ESTEC Contract No.22954/09) and the SMOS Soil Moisture Network Study—Operational Phase (ESA ESTEC Contract No.4000102722/10).

References

- Albergel, C., P. de Rosnay, C. Gruhier, J. Muñoz-Sabater, S. Hasenauer, L. Isaksen, Y. Kerr, and W. Wagner. 2012. Evaluation of remotely sensed and modelled

- soil moisture products using global ground-based in situ observations. *Remote Sens. Environ.* 118:215–226. doi:10.1016/j.rse.2011.11.017
- Albergel, C., C. Rüdiger, T. Pellarin, J.C. Calvet, N. Fritz, F. Froissard, D. Suquia, A. Petitpa, B. Piguet, and E. Martin. 2008. From near-surface to root-zone soil moisture using an exponential filter: An assessment of the method based on in-situ observations and model simulations. *Hydrol. Earth Syst. Sci.* 12:1323–1337. doi:10.5194/hess-12-1323-2008
- Balsamo, G., P. Viterbo, A. Beljaars, B. van den Hurk, M. Hirschi, A.K. Betts, and K. Scipal. 2009. A revised hydrology for the ECMWF Model: Verification from field site to terrestrial water storage and impact in the integrated forecast system. *J. Hydrometeorol.* 10:623–643. doi:10.1175/2008JHM1068.1
- Bartalis, Z., W. Wagner, V. Naeimi, S. Hasenauer, K. Scipal, H. Bonekamp, J. Figa, and C. Anderson. 2007. Initial soil moisture retrievals from the METOP-A Advanced Scatterometer (ASCAT). *Geophys. Res. Lett.* 34:L20401. doi:10.1029/2007GL031088
- Basara, J.B., and T.M. Crawford. 2000. Improved installation procedures for deep-layer soil moisture measurements. *J. Atmos. Ocean. Technol.* 17:879–884. doi:10.1175/1520-0426(2000)017<0879:IIPFDL>2.0.CO;2
- Bell, J.E., M.E. Palecki, W. Collins, J.H. Lawrimore, H.J. Diamond, R.D. Leeper, M.E. Hall, J. Kochendorfer, T.P. Meyers, T. Wilson, and B. Baker. 2012. Climate reference network soil moisture and temperature observations. *J. Hydrometeorol.*
- Beyrich, F., and W.K. Adam. 2007. Site and data report for the Lindenbergs Reference Site in CEOP—Phase I. In: Report of the German Weather Service. German Weather Service, Main Office. p. 55.
- Bircher, S., N. Skou, K.H. Jensen, J.P. Walker, and L. Rasmussen. 2012. A soil moisture and temperature network for SMOS validation in Western Denmark. *Hydrol. Earth Syst. Sci.* 16:1445–1463. doi:10.5194/hess-16-1445-2012
- Bogena, H.R., J.A. Huisman, C. Oberdorster, and H. Vereecken. 2007. Evaluation of a low-cost soil water content sensor for wireless network applications. *J. Hydrol.* 344:32–42. doi:10.1016/j.jhydrol.2007.06.032
- Brocca, L., S. Hasenauer, T. Lacava, F. Melone, T. Moramarco, W. Wagner, W. Dorigo, P. Matgen, J. Martínez-Fernández, P. Llorens, J. Latron, C. Martin, and M. Bittelli. 2011. Soil moisture estimation through ASCAT and AMSR-E sensors: An intercomparison and validation study across Europe. *Remote Sens. Environ.* 115:3390–3408. doi:10.1016/j.rse.2011.08.003
- Brocca, L., F. Melone, and T. Moramarco. 2008. On the estimation of antecedent wetness conditions in rainfall-runoff modelling. *Hydrol. Processes* 22:629–642. doi:10.1002/hyp.6629
- Brocca, L., F. Melone, T. Moramarco, and R. Morbidelli. 2009. Antecedent wetness conditions based on ERS scatterometer data. *J. Hydrol.* 364:73–87. doi:10.1016/j.jhydrol.2008.10.007
- Brocca, L., F. Melone, T. Moramarco, and R. Morbidelli. 2010. Spatial-temporal variability of soil moisture and its estimation across scales. *Water Resour. Res.* 46:W02516. doi:10.1029/2009WR008016
- Calvet, J.C., N. Fritz, F. Froissard, D. Suquia, A. Petitpa, and B. Piguet. 2008. In situ soil moisture observations for the CAL/VAL of SMOS: The SMOS-MIA network. In: International Geoscience and Remote Sensing Symposium. IGARSS, Barcelona, Spain. p. 1196–1199.
- Cappelaere, B., L. Descroix, T. Lebel, N. Boulain, D. Ramier, J.P. Laurent, G. Favreau, S. Boubakraoui, M. Boucher, I. Bouzou Moussa, V. Chaffard, P. Hieriaux, H.B.A. Issoufou, E. Le Breton, I. Mamadou, Y. Nazoumou, M. Oi, C. Ottlé, and G. Quantin. 2009. The AMMA-CATCH experiment in the cultivated Sahelian area of south-west Niger—Investigating water cycle response to a fluctuating climate and changing environment. *J. Hydrol.* 375:34–51. doi:10.1016/j.jhydrol.2009.06.021
- Congalton, R.G., and K. Green. 2009. Assessing the accuracy of remotely sensed data: Principles and practices. 2nd ed. CRC Press/Taylor and Francis, Boca Raton, FL.
- Dai, A., K.E. Trenberth, and T. Qian. 2004. A global dataset of Palmer Drought Severity Index for 1870–2002: Relationship with soil moisture and effects of surface warming. *J. Hydrometeorol.* 5:1117–1130. doi:10.1175/JHM-386.1
- DATA-MEQ. 2010. Recommendations for in-situ data, Near Real Time Quality Control, DATA-MEQ working group, EG10.19. In.
- de Rosnay, P., C. Gruhier, F. Timouk, F. Baup, E. Mougin, P. Hieriaux, L. Ker-goat, and V. LeDantec. 2009. Multi-scale soil moisture measurements at the Gourma meso-scale site in Mali. *J. Hydrol.* 375:241–252. doi:10.1016/j.jhydrol.2009.01.015
- Dee, D.P., S.M. Uppala, A.J. Simmons, P. Berrisford, P. Poli, S. Kobayashi, U. Andrae, M.A. Balmaseda, G. Balsamo, P. Bauer, P. Bechtold, A.C.M. Beljaars, L. van de Berg, J. Bidlot, N. Bormann, C. Delsol, R. Dragani, M. Fuentes, A.J. Geer, L. Haimberger, S.B. Healy, H. Hersbach, E.V. Hölm, L. Isaksen, P. Källberg, M. Köhler, M. Matricardi, A.P. McNally, B.M. Monge-Sanz, J.J. Mortreuil, B.K. Park, C. Peubey, P. de Rosnay, C. Tavolato, J.N. Thépaut, and F. Vitart. 2011. The ERA-Interim reanalysis: Configuration and performance of the data assimilation system. *Q. J. R. Meteorol. Soc.* 137:553–597. doi:10.1002/qj.828
- Derber, C.J., F.D. Parrish, and J.S. Lord. 1991. The new global operational analysis system at the National Meteorological Center. American Meteorological Society, Boston, MA.
- Dharssi, I., K.J. Bovis, B. Macpherson, and C.P. Jones. 2011. Operational assimilation of ASCAT surface soil wetness at the Met Office. *Hydrol. Earth Syst. Sci.* 15:2729–2746. doi:10.5194/hess-15-2729-2011
- Dorigo, W., P. Van Oevelen, W. Wagner, M. Drusch, S. Mecklenburg, A. Robock, and T. Jackson. 2011a. A New international network for in situ soil moisture data. *Eos Trans. AGU* 92:141–142. doi:10.1029/2011EO170001
- Dorigo, W.A., W. Wagner, R. Hohensinn, S. Hahn, C. Paulik, A. Xaver, A. Gruber, M. Drusch, S. Mecklenburg, P. van Oevelen, A. Robock, and T. Jackson. 2011b. The International Soil Moisture Network: A data hosting facility for global in situ soil moisture measurements. *Hydrol. Earth Syst. Sci.* 15:1675–1698. doi:10.5194/hess-15-1675-2011
- Entekhabi, D., E.G. Njoku, P.E. O'Neill, K.H. Kellogg, W.T. Crow, W.N. Edelstein, J.K. Entin, S.D. Goodman, T.J. Jackson, J. Johnson, J. Kimball, J.R. Piepmeier, R.D. Koster, N. Martin, K.C. McDonald, M. Moghaddam, S. Moran, R. Reichle, J.C. Shi, M.W. Spencer, S.W. Thurman, L. Tsang, and J. Van Zyl. 2010. The soil moisture active passive (SMAP) mission. *Proc. IEEE* 98:704–716. doi:10.1109/JPROC.2010.2043918
- Entin, J.K., A. Robock, K.Y. Vinnikov, S.E. Hollinger, S. Liu, and A. Namkhai. 2000. Temporal and spatial scales of observed soil moisture variations in the extratropics. *J. Geophys. Res. D Atmos.* 105:11865–11877. doi:10.1029/2000JD900051
- Famiglietti, J.S., D. Ryu, A.A. Berg, M. Rodell, and T.J. Jackson. 2008. Field observations of soil moisture variability across scales. *Water Resour. Res.* 44:W01423. doi:10.1029/2006WR005804
- FAO/IIASA/ISRIC/ISS-CAS/JRC. 2009. Harmonized World Soil Database. Version 1.1. FAO, Rome, Italy and IIASA, Laxenburg, Austria.
- Farrokhi, A., N. Talebi, and F. Safari. 2010. Automatic detection of epileptic spike using fuzzy ARTMAP neural network. In: Proceedings of the 10th WSEAS international conference on Signal processing, computational geometry and artificial vision. World Scientific and Engineering Academy and Society (WSEAS), Taipei, Taiwan. p. 64–66.
- González-Rouco, J.F., J.L. Jiménez, V. Quesada, and F. Valero. 2001. Quality control and homogeneity of precipitation data in the southwest of Europe. *J. Clim.* 14:964–978. doi:10.1175/1520-0442(2001)014<0964:QCAHOP>2.0.CO;2
- Gruhier, C., P. de Rosnay, S. Hasenauer, T. Holmes, R. de Jeu, Y. Kerr, E. Mougin, E. Njoku, F. Timouk, W. Wagner, and M. Zribi. 2010. Soil moisture active and passive microwave products: Intercomparison and evaluation over a Sahelian site. *Hydrol. Earth Syst. Sci.* 14:141–156. doi:10.5194/hess-14-141-2010
- Hallikainen, M.T., F.T. Ulaby, M.C. Dobson, M.A. El-Rayes, and L.-K. Wu. 1985. Microwave dielectric behavior of wet soil-Part I. Empirical models and experimental observations. *IEEE Trans. Geosci. Rem. Sens. GE-23:25–34.* doi:10.1109/TGRS.1985.289497
- Hillel, D. 1998. Environmental soil physics. Academic Press, San Diego.
- Hirschi, M., S.I. Seneviratne, V. Alexandrov, F. Boberg, C. Boroneant, O.B. Christensen, H. Formayer, B. Orłowsky, and P. Stepanek. 2011. Observational evidence for soil-moisture impact on hot extremes in southeastern Europe. *Nat. Geosci.* 4:17–21. doi:10.1038/ngeo1032
- Hollinger, S.E., and S.A. Isard. 1994. A soil moisture climatology of Illinois. *J. Clim.* 7:822–833. doi:10.1175/1520-0442(1994)007<0822:ASMCOI>2.0.CO;2
- Hubbard, K.G., S. Goddard, W.D. Sorenson, N. Wells, and T.T. Osugi. 2005. Performance of quality assurance procedures for an applied climate information system. *J. Atmos. Ocean. Technol.* 22:105–112. doi:10.1175/JTECH-1657.1
- Illston, B.G., J.B. Basara, D.K. Fisher, R. Elliott, C.A. Fiebrich, K.C. Crawford, K. Humes, and E. Hunt. 2008. Mesoscale monitoring of soil moisture across a statewide network. *J. Atmos. Ocean. Technol.* 25:167–182. doi:10.1175/2007JTECHA993.1
- Inan, Z.H., and M. Kuntalp. 2007. A study on fuzzy C-means clustering-based systems in automatic spike detection. *Comput. Biol. Med.* 37:1160–1166. doi:10.1016/j.combiomed.2006.10.010
- Ingleby, B., and M. Huddleston. 2007. Quality control of ocean temperature and salinity profiles- Historical and real-time data. *J. Mar. Syst.* 65:158–175. doi:10.1016/j.jmarsys.2005.11.019
- Jackson, T.J., M.H. Cosh, R. Bindlish, P.J. Starks, D.D. Bosch, M. Seyfried, D.C. Goodrich, M.S. Moran, and J.D. Du. 2010. Validation of Advanced Microwave Scanning Radiometer Soil Moisture Products. *IEEE Trans. Geosci. Rem. Sens.* 48:4256–4272. doi:10.1109/TGRS.2010.2051035
- Journée, M., and C. Bertrand. 2011. Quality control of solar radiation data within the RMB solar measurements network. *Sol. Energy* 85:72–86. doi:10.1016/j.solener.2010.10.021
- Joyce, R.J., J.E. Janowiak, P.A. Arkin, and P. Xie. 2004. CMORPH: A method that produces global precipitation estimates from passive microwave and infrared data at high spatial and temporal resolution. *J. Hydrometeorol.* 5:487–503. doi:10.1175/1525-7541(2004)005<0487:CAMTPG>2.0.CO;2
- Liu, Y.Y., W.A. Dorigo, R.M. Parinussa, R.A.M. De Jeu, W. Wagner, M.F. McCabe, J.P. Evans, and A.I.J.M. Van Dijk. 2012. Trend-preserving blending of passive and active microwave soil moisture retrievals. *Remote Sens. Environ.* 123:280–297. doi:10.1016/j.rse.2012.03.014
- Liu, Y.Y., R.M. Parinussa, W.A. Dorigo, R.A.M. De Jeu, W. Wagner, A.I.J.M. Van Dijk, M.F. McCabe, and J.P. Evans. 2011. Developing an improved soil mois-

- ture dataset by blending passive and active microwave satellite-based retrievals. *Hydrol. Earth Syst. Sci.* 15:425–436. doi:10.5194/hess-15-425-2011
- Loew, A., J.T. Dall'Amico, F. Schlenz, and W. Mauser. 2010. The Upper Danube soil moisture validation site: Measurements and activities. In: *Earth Observation and Water Cycle Conference*. ESA Special Publications, Rome.
- Malyshev, A.B., and I.B. Sudakova. 1995. Algorithm for the spikes detection in the cosmic ray intensity measurements from the data of satellite. *Geomagnet. Aerona.* 34:578–580.
- Marczewski, W., J. Slominski, E. Slominska, B. Usowicz, J. Usowicz, S. Romanov, O. Maryskevych, J. Nastula, and J. Zawadzki. 2010. Strategies for validating and directions for employing SMOS data, in the Cal-Cal project SWEX (3275) for wetlands. *Hydrol. Earth Syst. Sci. Discuss.* 7:7007–7057. doi:10.5194/hess-7-7007-2010
- Mecklenburg, S., M. Drusch, Y.H. Kerr, J. Font, M. Martin-Neira, S. Delwart, G. Buenadicha, N. Reul, E. Daganzo-Eusebio, R. Oliva, and R. Crapolichio. 2012. ESA's soil moisture and ocean salinity mission: Mission performance and operations. *IEEE Trans. Geosci. Rem. Sens.* 50:1354–1366. doi:10.1109/TGRS.2012.2187666
- Meinander, O., W. Josefsson, J. Kaurola, T. Koskela, and K. Lakkala. 2003. Spike detection and correction in Brewer spectroradiometer ultraviolet spectra. *Opt. Eng.* 42:1812–1819. doi:10.1117/1.1569492
- Merchant, C.J., P. Le Borgne, A. Marsouin, and H. Roquet. 2008. Optimal estimation of sea surface temperature from split-window observations. *Remote Sens. Environ.* 112:2469–2484. doi:10.1016/j.rse.2007.11.011
- Mittelbach, H., F. Casini, I. Lehner, A.J. Teuling, and S.I. Seneviratne. 2011. Soil moisture monitoring for climate research: Evaluation of a low-cost sensor in the framework of the Swiss soil moisture experiment (SwissSMEX) campaign. *J. Geophys. Res. D Atmos.* 116:D05111. doi:10.1029/2010JD014907
- Mougin, E., P. Hiernaux, L. Kergoat, M. Grippa, P. de Rosnay, F. Timouk, V. Le Dantec, V. Demarez, F. Lavenu, M. Arjounin, T. Lebel, N. Soumague, E. Ceschia, B. Mougenot, F. Baup, F. Frappart, P.L. Frison, J. Gardelle, C. Gruhier, L. Jarlan, S. Mangiarotti, B. Sanou, Y. Tracol, F. Guichard, V. Trichon, L. Diarra, A. Soumaré, M. Koité, F. Dembélé, C. Lloyd, N.P. Hanan, C. Damesin, C. Delon, D. Serça, C. Galy-Lacaux, J. Seghieri, S. Becerra, H. Dia, F. Gangneron, and P. Mazzeza. 2009. The AMMA-CATCH Gourma observatory site in Mali: Relating climatic variations to changes in vegetation, surface hydrology, fluxes and natural resources. *J. Hydrol.* 375:14–33. doi:10.1016/j.jhydrol.2009.06.045
- Nenadic, Z., and J.W. Burdick. 2005. Spike detection using the continuous wavelet transform. *IEEE Trans. Biomed. Eng.* 52:74–87. doi:10.1109/TBME.2004.839800
- Ossadtchi, A., S. Baillet, J.C. Mosher, D. Thyerlei, W. Sutherling, and R.M. Leahy. 2004. Automated interictal spike detection and source localization in magnetoencephalography using independent components analysis and spatio-temporal clustering. *Clin. Neurophysiol.* 115:508–522. doi:10.1016/j.clinph.2003.10.036
- Owe, M., R. de Jeu, and T. Holmes. 2008. Multisensor historical climatology of satellite-derived global land surface moisture. *J. Geophys. Res. Earth Surf.* 113:F01002. doi:10.1029/2007JF000769
- Parrens, M., E. Zakharova, S. Lafont, J.C. Calvet, Y. Kerr, W. Wagner, and J.P. Wigneron. 2012. Comparing soil moisture retrievals from SMOS and ASCAT over France. *Hydrol. Earth Syst. Sci.* 16:423–440. doi:10.5194/hess-16-423-2012
- Pathé, C., W. Wagner, D. Sabel, M. Doubkova, and J.B. Basara. 2009. Using ENVISAT ASAR global mode data for surface soil moisture retrieval over Oklahoma, USA. *IEEE Trans. Geosci. Rem. Sens.* 47:468–480. doi:10.1109/TGRS.2008.2004711
- Peel, M.C., B.L. Finlayson, and T.A. McMahon. 2007. Updated world map of the Köppen-Geiger climate classification. *Hydrol. Earth Syst. Sci.* 11:1633–1644. doi:10.5194/hess-11-1633-2007
- Peischl, S., J.P. Walker, C. Rüdiger, N. Ye, Y.H. Kerr, E. Kim, R. Bandara, and M. Allahmoradi. 2012. The AACES field experiments: SMOS calibration and validation across the Murrumbidgee River catchment. *Hydrol. Earth Syst. Sci.* 16:1697–1708. doi:10.5194/hess-16-1697-2012
- Pellarin, T., J.P. Laurent, B. Cappelaere, B. Decharme, L. Descroix, and D. Ramier. 2009. Hydrological modelling and associated microwave emission of a semi-arid region in South-western Niger. *J. Hydrol.* 375:262–272. doi:10.1016/j.jhydrol.2008.12.003
- Rautainen, K., J. Lemmettyinen, J. Pulliainen, J. Vehvilainen, M. Drusch, A. Kontu, J. Kainulainen, and J. Seppänen. 2012. L-band radiometer observations of soil processes in boreal and subarctic environments. *IEEE Trans. Geosci. Rem. Sens.* 50:1483–1497. doi:10.1109/TGRS.2011.2167755
- Rayner, N.A., P. Brohan, D.E. Parker, C.K. Folland, J.J. Kennedy, M. Vanicek, T.J. Ansell, and S.F.B. Tett. 2006. Improved analyses of changes and uncertainties in sea surface temperature measured in situ since the mid-nineteenth century: The HadSST2 dataset. *J. Clim.* 19:446–469. doi:10.1175/JCLI3637.1
- Robinson, D.A., C.S. Campbell, J.W. Hopmans, B.K. Hornbuckle, S.B. Jones, R. Knight, F. Ogden, J. Selker, and O. Wendroth. 2008. Soil moisture measurement for ecological and hydrological watershed-scale observatories: A review. *Vadose Zone J.* 7:358–389. doi:10.2136/vzj2007.0143
- Robock, A., K.Y. Vinnikov, G. Srinivasan, J.K. Entin, S.E. Hollinger, N.A. Speranskaya, S. Liu, and A. Namkhai. 2000. The Global Soil Moisture Data Bank. *Bull. Am. Meteorol. Soc.* 81:1281–1299. doi:10.1175/1520-0477(2000)081<1281:TGSMDB>2.3.CO;2
- Rodell, M., P.R. Houser, U. Jambor, J. Gottschalk, K. Mitchell, C.J. Meng, K. Arsenault, B. Cosgrove, J. Radakovitch, M. Bosilovich, J.K. Entin, J.P. Walker, D. Lohmann, and D. Toll. 2004. The Global Land Data Assimilation System. *Bull. Am. Meteorol. Soc.* 85:381–394. doi:10.1175/BAMS-85-3-381
- Rüdiger, C., G. Hancock, H.M. Hemakumara, B. Jacobs, J.D. Kalma, C. Martinez, M. Thyer, J.P. Walker, T. Wells, and G.R. Willgoose. 2007. Goulburn River experimental catchment data set. *Water Resour. Res.* 43:W10403. doi:10.1029/2006WR005837
- Sanchez, N., J. Martinez-Fernandez, A. Scaini, and C. Perez-Gutierrez. 2012. Validation of the SMOS L2 Soil Moisture Data in the REMEDHUS Network (Spain). *Geosci. Remote Sens. IEEE Trans.* 50:1602–1611. doi:10.1109/TGRS.2012.2186971
- Savitzky, A., and M.J.E. Golay. 1964. Smoothing and differentiation of data by simplified least squares procedures. *Anal. Chem.* 36:1627–1639. doi:10.1021/ac60214a047
- Saxton, K.E., and W.J. Rawls. 2006. Soil water characteristic estimates by texture and organic matter for hydrologic solutions. *Soil Sci. Soc. Am. J.* 70:1569–1578. doi:10.2136/sssaj2005.0117
- Su, Z., J. Wen, L. Dente, R. van der Velde, L. Wang, Y. Ma, K. Yang, and Z. Hu. 2011. The Tibetan Plateau observatory of plateau scale soil moisture and soil temperature (Tibet-Obs) for quantifying uncertainties in coarse resolution satellite and model products. *Hydrol. Earth Syst. Sci.* 15:2303–2316. doi:10.5194/hess-15-2303-2011
- Taylor, C.M., R.A.M. De Jeu, F. Guichard, P.P. Harris, and W.A. Dorigo. 2012. Afternoon rain more likely over drier soils. *Nature* 489:282–286. doi:10.1038/nature11377
- Torrence, C., and G.P. Compo. 1998. A Practical Guide to Wavelet Analysis. *Bull. Am. Meteorol. Soc.* 79:61–78. doi:10.1175/1520-0477(1998)079<0061:APGTWA>2.0.CO;2
- Vinnikov, K.Y., and I.B. Yeserkepova. 1991. Soil moisture: Empirical data and model results. *J. Clim.* 4:66–79. doi:10.1175/1520-0442(1991)004<0066:SMEDAM>2.0.CO;2
- Wang, F., L. Wang, T. Koike, H. Zhou, K. Yang, A. Wang, and W. Li. 2011. Evaluation and application of a fine-resolution global data set in a semiarid mesoscale river basin with a distributed biosphere hydrological model. *J. Geophys. Res.* 116:D21108. doi:10.1029/2011JD015990
- Wang, G., D. Garcia, Y. Liu, R. de Jeu, and A. Johannes Dolman. 2012. A three-dimensional gap filling method for large geophysical datasets: Application to global satellite soil moisture observations. *Environ. Model. Softw.* 30:139–142. doi:10.1016/j.envsoft.2011.10.015
- You, J., K.G. Hubbard, R. Mahmood, V. Sridhar, and D. Todey. 2010. Quality control of soil water data in applied climate information system-case study in Nebraska. *J. Hydrol. Eng.* 15:200–209. doi:10.1061/(ASCE)HE.1943-5584.0000174
- Young, R., J. Walker, N. Yeoh, A. Smith, K. Ellett, O. Merlin, and A. Western. 2008. Soil moisture and meteorological observations from the Murrumbidgee catchment. Department of Civil and Environmental Engineering, The University of Melbourne.
- Zreda, M., D. Desilets, T.P.A. Ferre, and R.L. Scott. 2008. Measuring soil moisture content non-invasively at intermediate spatial scale using cosmic-ray neutrons. *Geophys. Res. Lett.* 35:L21402. doi:10.1029/2008GL035655
- Zribi, M., M. Pardé, P. De Rosnay, F. Baup, N. Boulain, L. Descroix, T. Pellarin, E. Mougin, C. Ottlé, and B. Decharme. 2009. ERS scatterometer surface soil moisture analysis of two sites in the south and north of the Sahel region of West Africa. *J. Hydrol.* 375:253–261. doi:10.1016/j.jhydrol.2008.11.046